Author Manuscript

Author Manuscript

Author Manuscript

Author Manuscript

HHS Public Access

Author manuscript

Pharmacol Res. Author manuscript; available in PMC 2021 July 01.

Published in final edited form as:

Pharmacol Res. 2021 July ; 169: 105653. doi:10.1016/j.phrs.2021.105653.

Delineation of the functional properties exhibited by the Zinc-Activated Channel (ZAC) and its high-frequency Thr^{128}Ala variant (rs2257020) in *Xenopus* oocytes

Nawid Madjroh[a], **Paul A. Davies**[b], **Joshua L. Smalley**[b], **Uffe Kristiansen**[a], **Pella C. Söderhielm**[a], **Anders A. Jensen**[a,*]

[a]Department of Drug Design and Pharmacology, Faculty of Health and Medical Sciences, University of Copenhagen, 2100 Copenhagen Ø, Denmark

[b]Department of Neuroscience, Tufts University School of Medicine, Boston, MA, USA

Abstract

The signalling characteristics of the Zinc-Activated Channel (ZAC), a member of the Cys-loop receptor (CLR) superfamily, are presently poorly elucidated. The *ZACN* polymorphism c.454G>A encoding for the Thr^{128}Ala variation in ZAC is found in extremely high allele frequencies across ethnicities. In this, the first study of ZAC in *Xenopus* oocytes by TEVC electrophysiology, ZAC^{Thr128} and ZAC^{Ala128} exhibited largely comparable pharmacological and signalling characteristics, but interestingly the Zn^{2+}- and H^{+}-evoked current amplitudes in ZAC^{Ala128}-oocytes were dramatically smaller than those in ZAC^{Thr128}-oocytes. While the variation thus appeared to impact cell surface expression and/or channel properties of ZAC, the similar expression properties exhibited by ZAC^{Thr128} and ZAC^{Ala128} in transfected mammalian cells indicated that their distinct functionalities could arise from the latter. In co-expression experiments, wild-type and variant ZAC subunits assembled efficiently into "heteromeric" complexes in HEK293 cells, while the concomitant presence of ZAC^{Ala128} in ZAC^{Thr128}:ZAC^{Ala128}-oocytes did not exert a dominant negative effect on agonist-evoked current amplitudes compared to those in ZAC^{Thr128}-oocytes. Finally, the structural determinants of the functional importance of the 1-hydroxyethyl side-chain of Thr^{128} appeared to be subtle, as agonist-evoked current amplitudes in ZAC^{Ser128}-, ZAC^{Val128}- and ZAC^{Ile128}-oocytes also were substantially lower than those in ZAC^{Thr128}-oocytes. In conclusion, the functional properties exhibited by ZAC in this work substantiate the notion of it being an atypical CLR. While the impact of the Thr^{128}Ala variation on ZAC functionality in oocytes is striking, it remains to be investigated whether and to which extent this translates into an *in vivo* setting and thus could constitute a source of inter-individual variation in ZAC physiology.

*Corresponding author. aaj@sund.ku.dk (A.A. Jensen).

Declaration of Competing Interest

The authors declare that they have no known competing financial interests or personal relationships that could have appeared to influence the work reported in this paper.

Author Manuscript Author Manuscript Author Manuscript Author Manuscript

Keywords

Cys-loop receptor; Pentameric ligand-gated ion channel; Zinc-Activated Channel (ZAC); Two-electrode voltage clamp electrophysiology; Single nucleotide polymorphism (SNP); High-frequency variation

1. Introduction

The ligand-gated ion channels in the Cys-loop receptor (CLR) superfamily mediate the fast signalling of several important neurotransmitters [1]. The CLRs are homo- or heteromeric assemblies of five subunits, and the pentameric CLR complex is comprised by an extracellular domain (ECD), a transmembrane domain (TMD) and an intracellular domain made up by the N-termini, the four membrane-spanning α-helices, and the intracellular loops, respectively, of each of these five subunits [2–7]. Signal transduction through the CLR is triggered by agonist binding to orthosteric sites located in subunit interfaces of the ECD, which induces the opening of the ion channel comprised within the TMD and enables the flux of ions through it. The resulting signalling is eventually terminated either by deactivation and a return of the receptor to its resting, closed state or by desensitisation of the receptor into an agonist-bound, closed state [3,6–8].

The nicotinic acetylcholine, 5-HT_3 serotonin, γ-aminobutyric $acid_A$ and glycine receptors (nAChRs, 5-HT_3Rs, $GABA_A$Rs, and GlyRs, respectively) constitute the four subfamilies of classical CLRs in the superfamily [9–12], whereas the fifth mammalian CLR subfamily is comprised exclusively by the Zinc-Activated Channel (ZAC) [13–15]. Although the ZAC protein exhibits very low sequence homology (< 20% amino acid sequence identity) with the other superfamily members, it comprises most of the structural hallmark features of a CLR, including the signature Cys-loop motif in the subunit ECD [13]. In support of these structural similarities, heterologous expression of ZAC in HEK293 and COS-7 cells has been shown to result in the formation of functional cation-selective channels that are gated by zinc, copper and protons at potentially physiologically relevant concentration ranges (Zn^{2+} EC_{50}: 180–540 μM; Cu^{2+} EC_{50}: 4.0 μM; H^+ EC_{50}: pH 5.6), while being inhibited by extracellular Ca^{2+} and Mg^{2+} and by the promiscuous CLR antagonist tubocurarine (TC) [13,15]. Interestingly, the signalling properties displayed by ZAC in these patch-clamp recordings have differed substantially from those of other CLRs, with the channel exhibiting remarkably high levels of spontaneous activity, very low degrees of desensitisation and a substantial run-up of current amplitudes over time [13,15].

The nAChRs, 5-HT_3Rs, $GABA_A$Rs, and GlyRs mediate a plethora of physiological functions throughout the central nervous system and in the periphery and have been pursued as drug targets in a wide range of disorders over the years [9,12,16–22]. In light of the well-established physiological importance of its family members, ZAC has received surprisingly little attention to date. The human *ZACN* gene at chromosome 17q23 originates from the same ancestral gene as the nAChR and 5-HT_3R genes, but *ZACN* orthologs are only found in higher species genomes, and the absence of an orthologous gene in the rodent genome has severely hampered explorations of the native expression and the physiological roles of ZAC [13]. While ZAC expression has been demonstrated at the transcript level in human brain,

Author Manuscript Author Manuscript Author Manuscript Author Manuscript

pancreas, placenta, thyroid, prostate, trachea and stomach tissue [13,14], expression of the ZAC protein *in vivo* has yet to be consistently demonstrated, although immunostaining data in a recent patent suggests ZAC protein expression in human thymus and lymph organs [23]. Analogously, the indications about putative (patho)physiological roles of ZAC reported to date have been scarce and rudimentary [23–25].

Genetic variation across the general population and between different ethnic groups and individuals is known to have profound implications for physiology, pathophysiology and disease treatment. A plethora of different types of variations have been identified in numerous genes in all four subfamilies of classical CLRs, several of which that have been linked with different phenotypes or traits, channelopathies/disorders and disease treatment efficacy, including strong causal links between nAChR and $GABA_AR$ gene polymorphisms and various forms of epilepsy and between GlyR gene polymorphisms and hyperekplexia [10,21,26–28]. In the case of *ZACN*, in particular one variation stands out as potentially particular interesting in terms of its putative contributions to inter-individual differences in ZAC physiology (Fig. 1). The single nucleotide polymorphism (SNP) c.454G>A in exon 5 of *ZACN* (rs2257020, chr17:76080334, GRCh38.p12) encodes for a non-synonymous Thr-to-Ala variation in position 128 in the mature ZAC protein (position 152 in the precursor ZAC protein) (Fig. 1A). Residue 128 is located in the β6′ segment of β-strand β6, a short stretch of 6 residues connecting the "loop E" segment of β6 to the Cys-loop (loop β6-β7) in the ECD of the ZAC subunit (Fig. 1B). This *ZACN* variation is found in such remarkably high allele frequencies in all ethnicities that heterozygous carriers of c.454A and c.454G alleles constitute the most abundant expected genotype in almost all populations studied (Fig. 1C and D, NCBI dbSNP, build 154, rs2257020 [29]). While the striking abundance of this SNP makes a distinction between major and minor alleles somewhat academic, c.454A and c.454G constitute the major and the minor allele in almost all ethnicities with allele frequencies in the 0.55–0.65 and 0.35–0.45 ranges, respectively, in most studies (Fig. 1C, NCBI dbSNP, build 154, rs2257020). In the present work, we will thus refer to ZAC^{Thr128} and ZAC^{Ala128} as the wild-type (WT) and variant ZAC, respectively.

In this, the first study of ZAC expressed in *Xenopus* oocytes by two-electrode voltage-clamp (TEVC) electrophysiology, we delineate the functional properties exhibited by ZAC^{Thr128} and ZAC^{Ala128} in detail and investigate the molecular and cellular basis for a striking difference in functionality observed between the WT ZAC and its high-frequency variant in this expression system.

2. Materials and methods

2.1. Materials

$ZnCl_2$ (0.1 M solution buffered at pH 7.4, catalogue number 39059), $CuCl_2$ and all chemicals for buffers were purchased from Sigma-Aldrich (St. Louis, MO), and culture medium, serum, antibiotics and trypsin for cell culture were obtained from Invitrogen (Paisley, UK). TC was purchased from Tocris Cookson (Bristol, UK), and the pUNIV vector was obtained from Addgene (Watertown, MA). Defolliculated stage V-VI oocytes harvested from female *Xenopus laevis* frogs were obtained from Lohmann Research Equipment (Castrop-Rauxel, Germany) and from an in-house facility. The care and use of *Xenopus*

Author Manuscript Author Manuscript Author Manuscript Author Manuscript

laevis from the in-house facility was in strict adherence to a protocol (license 2014-15-0201-00031) approved by the Danish Veterinary and Food Administration, in accordance with the Guide for the Care and Use of Laboratory Animals adopted by the U.S. National Institutes of Health.

2.2. Molecular biology

The construction of the WT ZAC-pCIneo (ZAC^{Thr128}-pCIneo) and HA-5-HT3B-pCIneo plasmids has been reported previously [15,30]. The ZAC^{Thr128} cDNA was subcloned into the pUNIV vector using the unique restriction enzymes *Nhe*I and *EcoR*I. The HA-ZAC^{Thr128}-pCIneo and myc-ZAC^{Thr128}-pCIneo constructs were generated by use of the overlap extension PCR technique [31] by insertion of the nucleotide sequence for the hemagglutinin (HA) epitope (Tyr-Pro-Tyr-Asp-Val-Pro-Asp-Tyr-Ala) or for the myc epitope (Glu-Gln-Lys-Leu-Ile-Ser-Glu-Glu-Asp-Leu) between the nucleotide sequences for the predicted signal peptide and the mature ZAC protein (…His-Gly-l-Gln-Gly…) in ZAC-pCIneo. The mutations in the various ZAC^{Ala128}, ZAC^{Ser128}, ZAC^{Val128}, ZAC^{Ile128} and ZAC^{Phe128} plasmids were introduced using the QuikChange mutagenesis kit (Stratagene, Santa Clara, CA) and oligonucleotides from TAG Copenhagen A/S (Copenhagen, Denmark). The codons encoding for Thr^{128} (ACC) and Ala^{128} (GCC) in all ZAC^{Thr128} and ZAC^{Ala128} cDNAs were the same as those in the c.454A and c.454G alleles of *ZACN*, respectively (Fig. 1A). The integrity and the absence of unwanted mutations in all cDNAs created by PCR were verified by DNA sequencing (Macrogen Europe, Amsterdam, The Netherlands).

2.3. Xenopus laevis oocytes and TEVC recordings

All cDNAs used for cRNA synthesis were in the pUNIV vector. The cDNAs were linearised and subsequently transcribed and capped using the mMessage mMachine T7 RNA transcription kit (Ambion, Waltham, MA). Stocks of 0.05 μg/μL were prepared for almost all cRNAs, and volumes of 4.6–36.8 nL were injected into the oocytes. 1.84 ng cRNA was injected into oocytes in most of the experiments with ZAC^{Thr128} and ZAC^{Ala128} and for all experiments with ZAC^{Ser128}, ZAC^{Val128}, ZAC^{Ile128} and ZAC^{Phe128}. For the studies of current amplitudes in oocytes with different ZAC^{Thr128} and ZAC^{Ala128} expression levels, ranges of 0.46–1.84 ng ZAC^{Thr128} cRNA and 0.92–3.68 ng ZAC^{Ala128} cRNA were injected. For the ZAC^{Thr128}/ZAC^{Ala128} co-expression studies, ZAC^{Thr128}:ZAC^{Ala128} cRNA ratios of 1:3, 1:1 and 3:1 (0.46:1.38, 0.92:0.92 and 1.38:0.46 ng, total cRNA: 1.84 ng) were injected into the oocytes. For controls in these experiments, the ZAC^{Ala128} cRNA was substituted with water, and oocytes were injected with the same quantities of ZAC^{Thr128} cRNA on its own (0.46, 0.92 and 1.38 ng). Oocytes were incubated in a sterile modified Barth's solution [88 mM NaCl, 1 mM KCl, 15 mM HEPES (pH 7.5), 2.4 mM $NaHCO_3$, 0.41 mM $CaCl_2$, 0.82 mM $MgSO_4$, 0.3 mM $Ca(NO_3)_2$, 100 U/ml penicillin and 100 μg/ml streptomycin] at 16–18 °C, and unless otherwise specified the oocytes were used 2 days after the injection.

On the day of experiment, all compound dilutions were prepared in a saline solution [115 mM NaCl, 2.5 mM KCl, 10 mM MOPS (pH 7.5), 1.8 mM $CaCl_2$, 0.1 mM $MgCl_2$] and pH was adjusted to 7.5 (if needed). Thus, with exception of those applying H^+ as ZAC agonist, all TEVC recordings were performed at pH 7.5. Oocytes were placed in a recording chamber

Author Manuscript Author Manuscript Author Manuscript Author Manuscript

continuously perfused with this saline solution, and the compounds were applied in the perfusate. Both voltage and current electrodes were agar-plugged with 3 M KCl with a resistance of 0.2–2.0 MΩ. Oocytes were voltage-clamped at − 50 mV (unless otherwise stated) by a Gene Clamp 500B amplifier and current signals were digitised by a Digidata 1322A (both from Axon Instruments, Union City, CA). Currents were recorded using pCLAMP 10 (Molecular Devices, Sunnyvale, CA). The recordings were performed at room temperature.

In all recordings, compounds or compound combinations were applied in the bath until the peak current decayed to a steady state (up to 30 s). To be able to determine a complete agonist concentration-response relationship on an oocyte, the maximal current evoked by each agonist concentration within a 30 s-application period was extracted as the data. While this admittedly represents an approximation, we argue that the true pharmacological properties of ZAC ligands are well reflected by this data analysis. At the beginning or end (whenever appropriate) of all recordings determining concentration-response relationships at ZAC, two consecutive applications of an agonist concentration giving rise to a maximal agonist-induced current (I_{max}) were applied on the oocyte, and it was verified that these consecutive applications elicited responses of comparable current amplitudes (±20%). The antagonist properties of TC at ZAC were determined by pre-application of TC to the perfusate 30 s followed by co-application of TC and the agonist. In all recordings, washes of 1–5 min were executed between the ligand applications, the length of the washes depending on the receptor kinetics and the “stickiness” of the compounds and on the compound concentrations used. In the studies comparing the current amplitudes evoked by Zn^{2+} and H^{+} in oocytes expressing ZAC^{Ala128} or other ZAC mutants or in uninjected oocytes with the currents evoked in oocytes expressing WT ZAC (ZAC^{Thr128}), the data were obtained from same batches of oocytes at the same day of experiments and using the same incubation times and the same cRNA amounts (unless otherwise stated).

The current-voltage (I-V) relationships exhibited by 1 mM Zn^{2+} and by 100 μM TC at WT ZAC in oocytes was studied by recordings of the current responses induced by the application of the respective drugs, applied for 30 s before actual recordings were initiated, at −60 to + 60 mV with a Δ20 mV voltage jump between each recording. Recordings were subsequently subtracted to baseline recordings (by perfusing with buffer) at same voltages.

2.4. Enzyme-linked immunosorbent assay (ELISA)

The total and cell surface expression levels of HA-tagged ZAC^{Thr128} and ZAC^{Ala128} subunits transiently expressed in tsA201 cells were quantified using an ELISA. The tsA201 cells (a transformed HEK293 cell line [32]) were cultured in GlutaMAX-I Dulbecco’s Modified Eagle’s Medium supplemented with 10% foetal bovine serum, penicillin (100 U/ml) and streptomycin (100 μg/ml) in a humidified atmosphere of 5% CO_2 at 37 °C. Exponentially growing tsA201 cells were split out into 6 cm tissue culture dishes (1×10^6 cells/dish) and transfected 22–24 h later using PolyFect (Qiagen, West Sussex, UK) according to the manufacturer’s protocol. All 6 cm dishes were transfected with a total of 4 μg cDNA, where “empty” pCIneo vector was used to fill up the cDNA amount to this quantity in all transfections: pCIneo (4 μg, control), HA-ZAC^{Thr128}-pCIneo (4.0 μg, control

Author Manuscript Author Manuscript Author Manuscript Author Manuscript

used for normalisation), HA-ZAC^{Thr128}-pCIneo (0.0625, 0.25, 1.0 or 4.0 μg), HA-ZAC^{Ala128}-pCIneo (0.0625, 0.25, 1.0 or 4.0 μg), HA-ZAC^{Thr128}-pCIneo/ZAC^{Ala128}-pCIneo (1.0/1.0 μg), HA-ZAC^{Ala128}-pCIneo/ZAC^{Thr128}-pCIneo (1.0/1.0 μg), HA-ZAC^{Thr128}-pCIneo/ρ1-pCIneo (1.0/1.0 μg), HA-ZAC^{Ala128}-pCIneo/ρ1-pCIne-pCIneo (1.0/1.0 μg), HA-5-HT3B-pCIneo (2.0 μg) or HA-5-HT3B-pCIneo/5-HT3A-pCIneo (2.0/2.0 μg).

16–18 h after the transfection, the cells were plated into PDL-coated 48-well plates (1×10^5 cells/well). The ELISA experiment was initiated 24–25 h after the plating of the cells, and it was performed essentially as previously described [30,33]. The cells were washed two times with ice-cold wash buffer (phosphate-buffered saline supplemented with 1 mM $CaCl_2$) and incubated in an ice-cold 4% paraformaldehyde solution for 12 min on ice, after which the following steps were performed at room temperature. The cells were washed four times with wash buffer, incubated for 30 min in blocking solution (3% dry milk in 50 mM Tris-HCl, 1 mM $CaCl_2$, pH 7.5), and incubated with rat monoclonal anti-HA-peroxidase conjugated antibody (clone 3F10, Sigma-Aldrich, diluted 1:1000 in blocking solution) for 1 h. Cells were then washed four times with washing buffer, and expression of the HA-tagged proteins was quantified using 3,3′,5,5′-tetramethylbenzidine liquid substrate system (Sigma Aldrich) and H_2SO_4. The absorbance of the supernatants was determined at 450 nm. Total expression levels of the HA-tagged proteins in the cells were determined by adding 0.1% Triton X-100 in the blocking solution used during the blocking and antibody incubation steps. All experiments were performed in triplicate, and data are based on a total of three independent experiments.

2.5. Co-immunoprecipitation assay

HEK293 cells were transfected with myc-ZAC^{Thr128}, myc-ZAC^{Thr128}/HA-ZAC^{Thr128} (1:1 ratio), myc-ZAC^{Thr128}/HA-ZAC^{Ala128} (1:1 ratio) or myc-ZAC^{Ala128}/HA-ZAC^{Ala128} (1:1 ratio) cDNAs by electroporation using a Bio-Rad Gene Pulser Xcell system (10 μg of each cDNA in 1×10^6 cells per condition). After 48 h, the cells were lysed in Triton lysis buffer (150 mM NaCl, 10 mM Tris, 0.5% Triton X-100, pH 7.5), and a Bradford assay was carried out to determine protein concentration. 250 μg of protein adjusted to equal volumes for each sample was loaded onto 50 μL of myc-Dynabeads (ThermoFisher) pre-washed with PBS-Tween (0.05%) and incubated at 4 °C on a daisywheel overnight. Unbound (flow through) material was saved and the beads washed with PBS-Tween. Bound material was eluted from the beads by incubating in 2x sample buffer (Sigma-Aldrich) at 55 °C. Immunoblots were carried out as previously described [34]. Briefly, samples were boiled for 5 min at 95 °C and 20 μg of protein loaded onto polyacrylamide gels for sodium dodecyl sulphate–poly acrylamide gel electrophoresis (SDS-PAGE). Proteins were then transferred onto nitrocellulose membranes, blocked in milk for 1 h, and probed with primary antibodies overnight; β-actin (Sigma-Aldrich, catalogue number A1978), myc (Santa-Cruz, catalogue number SC-40) and HA (Cell Signalling, catalogue number 2367). The membranes were washed in TBS-T (137 mM NaCl, 20 mM Tris, 0.1% Tween, pH 7.6) and probed with appropriate horseradish peroxidase-conjugated secondary antibodies and developed with enhanced chemiluminescent substrate in a Bio-Rad ChemiDoc Imager.

Author Manuscript Author Manuscript Author Manuscript Author Manuscript

2.6. Data and statistical analysis

Data analysis and statistical analysis of the data from the TEVC recordings were performed using Clampfit software version 10.5 (Molecular Devices, Crawley, UK) and GraphPad Prism version 7.0c (GraphPad Software, La Jolla, CA). Unless otherwise stated, the inward currents induced by ZAC agonists and the apparent outward currents induced by TC (which arise from a suppression of spontaneous ZAC activity) at ZAC-expressing oocytes were normalised to the maximal response elicited by a specific agonist (agonist I_{max}) on each oocyte. For the determination of the concentration-inhibition relationship of TC at ZAC, the current responses induced by 1 mM Zn^{2+} in the presence of various TC concentrations were normalised to that induced by Zn^{2+} on its own ($I_{1mM\ Zn2+}$). For the determination of the concentration-response relationships of Zn^{2+} in the presence of various TC concentrations, the current responses were normalised to the response evoked by 10 mM Zn^{2+} on each oocyte ($I_{10mM\ Zn2+}$). Concentration-response and concentration-inhibition curves were fitted in GraphPad Prism by nonlinear regression using the equation for sigmoidal dose-response with variable slope. I-V relationships were analysed by fitting the curves with a third order polynomium. Each data point represents the mean ± S.E.M. value of recordings performed on at least five oocytes in total from at least two different batches. For the data where statistical analysis was performed, a one-way ANOVA was used. The null hypothesis was rejected at $P < 0.05$, and the differences between the means were analysed by Tukey's multiple comparisons test.

For the ELISA data, the average absorbance in the wells with tsA201 cells transfected with pCIneo (4.0 μg, control) were subtracted from the absorbance measured in all other wells, which subsequently were normalised to the cell surface expression measured in the wells with cells transfected with HA-ZAC^{Thr128}-pCIneo (4.0 μg, control).

2.7. Construction of a homology model of ZAC

A ZAC homology model was generated based on published high-resolution structures of other CLRs as templates by use of the Phyre2 software [35]. The pentameric ZAC model was created based on an alignment of the amino acid sequences of ZAC and the murine 5-HT3A subunit in the Chimera software [36]. The homology model was not refined further, and it is exclusively used for illustration purposes.

3. Results

3.1. Implementation of functional studies of ZAC expressed in Xenopus oocytes by TEVC recordings

While previous patch-clamp recordings of ZAC signalling in HEK293 or COS-7 cells have provided insight into the biophysical, ion permeability and conductance properties of the channel, functional expression of ZAC in mammalian cells and data generation in this set-up was also found not to be trivial and to be quite laborious [13,15]. In order to enable the studies of ZAC presented here, we thus applied the *Xenopus* oocyte expression system and TEVC recordings, a robust functional assay for studies of recombinant ion channels and other electrogenic proteins [37,38].

Author Manuscript Author Manuscript Author Manuscript Author Manuscript

To assess the suitability of *Xenopus* oocytes as expression system for ZAC and to investigate for non-specific responses produced by applications of the ZAC agonists on these cells, we initially compared the current responses evoked by Zn^{2+}, Cu^{2+} and H^+ in oocytes injected with WT ZAC (ZAC^{Thr128}) cRNA and in uninjected oocytes (Fig. 2). Both Zn^{2+} and H^+ elicited robust inward current responses in ZAC-expressing oocytes in a concentration-dependent manner (Fig. 2A and B), with current amplitudes evoked by protons consistently being significantly higher than those induced by Zn^{2+} in all batches of oocytes tested throughout the study. Application of higher Zn^{2+} and H^+ concentrations than 10 mM and pH 3.5, respectively, resulted in non-specific currents and oocyte instability (data not shown). In comparison to the currents recorded from ZAC-oocytes, Zn^{2+} (0.01–10 mM) did not evoke significant responses in uninjected oocytes, and the proton-evoked currents (pH 6.5–3.5) in these oocytes were minute, with pH 3.5 evoking current amplitudes in the 30–52 nA range, respectively (Fig. 2A and B). Importantly, the negligible H^+-evoked currents in uninjected oocytes were not significantly reduced by the presence of ZAC antagonist TC (100 μM), in contrast to the robust TC-mediated inhibition of proton-induced responses in ZAC-expressing oocytes (Fig. 2B). Thus, the minute proton-evoked currents in uninjected oocytes clearly arose from a different origin than the vastly higher amplitudes recorded from ZAC-expressing oocytes and could be pharmacologically distinguished from these.

Applications of Cu^{2+} (10–1000 μM) at ZAC-expressing oocytes also elicited currents of substantial amplitudes, whereas the metal ion did not induce significant responses in uninjected oocytes (Fig. 2C). However, the Cu^{2+}-evoked response through ZAC were characterised by a substantial tail current and a much slower return to baseline following termination of Cu^{2+} application than observed for the Zn^{2+}- and H^+-induced currents (Fig. 2C). Moreover, repeated applications of Cu^{2+}, in particular at 100–1000 μM concentrations, resulted in oocyte instability and eventually failure to maintain the clamp (data not shown). Because of this, it was not possible to determine a complete concentration-response relationship for Cu^{2+} at ZAC at one oocyte, and thus we decided only to use Zn^{2+} and H^+ as ZAC agonists in the rest of this study.

We next investigated the functional expression of ZAC in the oocytes over time following injection of 1.84 ng cRNA. As exemplified for Zn^{2+} (10 mM) in Fig. 2D, only small agonist-induced currents could be measured in the oocytes the day after cRNA injection, whereas robust ZAC-mediated currents were recorded consistently in the oocytes from Day 2 to Day 6 after injection. However, the visual appearance and overall wellbeing of the oocytes as well as the profiles and reproducibility of the current responses recorded from the ZAC-expressing oocytes changed substantially over these 5 days. In recordings on Day 2 after the cRNA injection, we consistently observed Zn^{2+}- and H^+-evoked current profiles as exemplified in Fig. 2A and B, with very little variation between the current amplitudes induced by repeated applications of the same agonist concentration over the duration of a 10–15 min recording period (data not shown). Thus, we did not observe a run-up of agonist-induced current amplitudes in ZAC-expressing oocytes as observed in previous patch-clamp recordings from ZAC-expressing mammalian cells, but it should be stressed that the recordings in these patch-clamp studies were performed for up to 1 h [13,15]. In contrast to the consistency of the recorded data from ZAC-oocytes on Day 2, from Day 3 and forward, the health of the ZAC-expressing oocytes appeared to deteriorate, which also impacted the

Author Manuscript Author Manuscript Author Manuscript Author Manuscript

quality of the currents recorded from them noticeably. The fraction of “soft” and leaky oocytes increased substantially over Days 3–6, and in the recordings from ZAC-oocytes during these 4 days we consistently observed more negative baseline currents, highly leaked currents, failure of the agonist-evoked currents to return to baseline even after several min of washing with buffer, and failure to maintain the clamped potential at − 50 mV over the course of an experiment. Collectively, these characteristics meant that it was not possible to determine a complete and reliable agonist concentration-response relationship in recordings on a single oocyte on Days 3–6, and consequently all TEVC recordings in this work were performed on oocytes 2 days after cRNA injection.

3.2. Functional properties displayed by WT ZAC in Xenopus oocytes

Initially, the functional properties of WT ZAC (ZAC^{Thr128}) were characterised in detail and compared to those displayed by the receptor in previous patch-clamp recordings [13,15].

3.2.1. Agonist pharmacology—Zn^{2+} induced current responses in a concentration-dependent manner in ZAC^{Thr128}-expressing oocytes, exhibiting an average EC_{50} value of 1.0 mM (pEC_{50} ± S.E.M.: 2.98 ± 0.07, n = 6) and an average Hill coefficient of 2.2 ± 0.1 (mean ± S.E.M, n = 6) (Fig. 3A). Thus, the agonist potency displayed by Zn^{2+} in these recordings was 2- and 5-fold lower than those determined for the metal ion in patch-clamp recordings from ZAC-expressing HEK293 and COS-7 cells, respectively, whereas the Hill coefficient of its concentration-response relationship was essentially the same as in these previous studies [13,15].

In contrast to the consistency of the functional properties displayed by Zn^{2+} as ZAC agonist, H^+ exhibited two very distinct profiles at ZAC-expressing oocytes. In the majority of oocytes (~75%), application of H^+ concentrations yielding pH values ranging from 6.0 to 3.5 produced significant currents in a concentration-dependent manner and a concentration-response relationship that had not plateaued at pH 3.5 (Fig. 3B). In contrast, H^+ was a much more potent agonist at other ZAC-oocytes (~25%), exhibiting a complete concentration-response relationship characterised by an EC_{50} of 1.0 μM (pEC_{50}/pH_{50} S.E.M.: 5.99 ± 0.02, n = 7) and a Hill coefficient of 1.96 ± 0.26 (mean ± S.E.M., n = 7) (Fig. 3B). Interestingly, the potency exhibited by H^+ at these oocytes was in concordance with that observed in patch-clamp studies of ZAC in COS-7 cells (pH 5.6) [15]. The “low-potency” and “high-potency” H^+ profiles were found to be exclusively attributable to batch-to-batch variation in the oocytes, as very low oocyte-to-oocyte variability within each batch were observed, where the H^+ concentration-response relationships were very similar and all could be classified as either “low-potency” or “high-potency” (depending on the oocyte batch). No clear correlation seemed to exist between the level of ZAC expression (assessed by the recorded current amplitudes) or the levels of spontaneous activity exhibited by ZAC (assessed by TC (100 μM)-evoked current amplitudes) in the oocytes and the observed H^+ profiles. Importantly, TC inhibited the proton-evoked responses in oocytes exhibiting both H^+ profiles with comparable IC_{50} values, demonstrating that both the “low-potency” and “high-potency” responses were mediated through ZAC (Fig. 2B and data not shown). Notably, Zn^{2+} exhibited comparable EC_{50} values at oocytes exhibiting both “low-potency” or “high-potency” H^+ profiles.

Author Manuscript Author Manuscript Author Manuscript Author Manuscript

3.2.2. Channel properties—As outlined in Section 1, the channel characteristics exhibited by ZAC expressed in mammalian cells differ substantially from those of other CLRs [13,15]. Although TEVC recordings from oocytes do not allow for extraction of reliable information about kinetic properties of channels, the current responses evoked by Zn^{2+} and H^+ in ZAC-expressing oocytes nevertheless seemed to reflect the previously reported kinetic properties of the receptor [13,15]. The rise phase of the agonist-induced ZAC current was very slow, and only at saturating Zn^{2+} concentrations currents reached well defined peaks within the application period of 30 s (Fig. 3A and B). In fact, the currents evoked by sustained application of sub-saturating concentrations of Zn^{2+} or H^+ did not reach completely established peaks within the time periods investigated (up to 4 min for Zn^{2+} and up to 90 s for H^+) (Fig. 3C). While this observation in part could be due to slow activation kinetics, it is mostly rooted in the very slow desensitisation of ZAC also observed in the patch-clamp studies [13,15], with current decay during agonist application only being observed at the highest agonist concentrations (Fig. 3A–C). In contrast, the rapid decay of the current responses observed upon termination of agonist application indicated that deactivation kinetics of ZAC are fast (Fig. 3A and B), which aligns well with the fast decay kinetics exhibited by Zn^{2+} and in particular H^+ in patch-clamp recordings from ZAC-expressing COS-7 cells [15].

We also investigated the I-V relationship exhibited by ZAC by recording the currents evoked by 1 mM Zn^{2+} (~EC_{50}) at holding potentials ranging from − 60 mV to + 60 mV (Fig. 3D). The amplitudes of the Zn^{2+}-induced currents were considerably higher at positive than at corresponding negative potentials and were thus characterised by outward rectification, and the reversal potential determined for Zn^{2+} was − 8.8 mV. Thus, the I-V relationship and the reversal potential displayed by the metal ion at ZAC in oocytes were in excellent agreement with those determined in patch-clamp recordings from ZAC-expressing HEK293 cells [13].

3.2.3. Antagonist pharmacology of TC and spontaneous ZAC activity—The TC-mediated ZAC antagonism observed in a previous patch-clamp study [13] was next verified at ZAC-expressing oocytes (Fig. 4). TC mediated concentration-dependent inhibition of Zn^{2+} (1 mM)-evoked currents in the oocytes exhibiting an IC_{50} value of 3.2 μM (pIC_{50} ± S.E.M.: 5.49 ± 0.04, n = 8), a 2-fold lower value than its IC_{50} at ZAC in the patch-clamp recordings (Fig. 4A) [13]. The mechanism underlying the TC-mediated ZAC inhibition was investigated by determination of the concentration-response relationships for Zn^{2+} at the receptor in the absence and presence of various TC concentrations (Fig. 4B). The maximal current response evoked by Zn^{2+} in ZAC-expressing oocytes was progressively reduced with increasing TC concentrations. Since the Zn^{2+} concentration-response relationships obtained in the presence of TC were not completely saturated in the Zn^{2+} concentration ranges tested, EC_{50} values could not be reliably extracted from them. However, visual inspection of the concentration-response curves suggests that the potency of Zn^{2+} is somewhat reduced by the presence of TC. Nevertheless, the TC-mediated antagonism of ZAC appeared to be largely non-competitive in its nature (Fig. 4).

ZAC has previously been shown to exhibit substantial levels of spontaneous activity in mammalian cells through the use of its antagonists TC and Ca^{2+} [13,15]. Analogously, TC inhibited the spontaneous activity of ZAC in oocytes in a concentration-dependent manner

Author Manuscript Author Manuscript Author Manuscript Author Manuscript

exhibiting an IC_{50} value of 3.3 μM (pIC_{50} ± S.E.M.: 5.48 ± 0.03, n = 5, Fig. 4C), which was very similar to its potency as an antagonist of Zn^{2+}-mediated ZAC signalling (Fig. 4A). The size of the spontaneous ZAC activity varied somewhat between oocytes, with the current amplitude evoked by TC (100 μM) constituting between 1% and 10% of that evoked by Zn^{2+} (10 mM) (Fig. 4C). The I-V relationship of the TC-mediated block of spontaneous ZAC activity was characterised in recordings using 100 μM TC and holding potentials between − 60 mV and + 60 mV (Fig. 4D). The apparent currents arising from the TC-mediated block of the spontaneous ZAC activity were characterised by considerably higher amplitudes at positive than at corresponding negative potentials, indicating that the spontaneous currents were outwardly rectifying. Both the I-V relationship and the reversal potential (− 6.3 mV) determined for TC were in excellent agreement with those determined in patch-clamp recordings from ZAC-expressing HEK293 cells [13].

3.3. Functional properties displayed by the ZAC^{Ala128} variant in Xenopus oocytes

As outlined in Section 1, the c.454G>A SNP in the open reading frame of *ZACN* (rs2257020) is found in remarkably high allele frequencies in the general population (Fig. 1A and B). In light of the putative importance of this SNP for ZAC physiology, we decided to investigate the impact of the resulting non-synonymous $Thr^{128}Ala$ variation on the functionality of recombinant ZAC expressed in oocytes.

Introduction of the $Thr^{128}Ala$ substitution in ZAC was observed to have dramatic implications for the size of the agonist-induced response through the receptor. In oocytes from the same batches injected with the same quantities (1.84 ng) of ZAC^{Thr128} or ZAC^{Ala128} cRNA and incubated under the same conditions and time periods until the recordings, the current amplitudes evoked by both Zn^{2+} (1 mM) and H^+ (pH 4.0) through ZAC^{Ala128}-oocytes were dramatically smaller than those produced by the two agonists in ZAC^{Thr128}-oocytes (Fig. 5A and B). Albeit small, the amplitudes of Zn^{2+}- and H^+-evoked currents in ZAC^{Ala128}-oocytes were significantly higher than those in uninjected oocytes (Fig. 5A and B, *left*). In support of these currents in ZAC^{Ala128}-oocytes being mediated through cell surface-expressed receptors, TC (100 μM) was found to inhibit the Zn^{2+} (10 mM)-induced responses in these oocytes significantly (Fig. 5B, *right*).

The markedly lower current amplitudes recorded from ZAC^{Ala128} compared to ZAC^{Thr128} in oocytes on Day 2 after cRNA injection could potentially be rooted in a longer time course for functional expression of the variant than for the WT receptor. To investigate this possibility, we characterised the functional expression of ZAC^{Ala128} in oocytes in the six days following injection of 1.84 ng cRNA (Fig. 5C), recordings performed in parallel to the analogous recordings for ZAC^{Thr128} (Fig. 2D). Qualitatively very similar to the expression-over-time profile exhibited by the WT ZAC in these experiments, only low levels of functional expression of ZAC^{Ala128} could be detected in the oocytes on Day 1 after the cRNA injection, whereas significantly higher Zn^{2+} (10 mM)-evoked current amplitudes were observed starting from Day 2 and the following four days (Fig. 5C, *left*). Importantly, the largely comparable amplitudes recorded from ZAC^{Ala128}-oocytes over these 5 days were consistently lower than those recorded from ZAC^{Thr128}-oocytes on the same day, with ratios between the averaged ZAC^{Thr128} and ZAC^{Ala128} $I_{10mM\ Zn2+}$ values on Days 2, 3, 4, 5 and 6

Author Manuscript Author Manuscript Author Manuscript Author Manuscript

being 23, 15, 20, 16 and 16, respectively (Fig. 5C, *right*). In light of this, the observed distinct WT and variant ZAC functionalities in the oocytes did not seem to arise from time-differential patterns of expression of the two receptors. For the subsequent comparisons of WT and variant ZAC signalling in the oocytes in this work, we performed all TEVC recordings on both ZAC^{Thr128}- and ZAC^{Ala128}-oocytes 2 days after cRNA injection.

The differences in agonist-induced current amplitudes in ZAC^{Thr128}- and ZAC^{Ala128}-oocytes were next elucidated further by a systematic investigation of the correlation between the quantities of cRNAs for the two subunits injected into the oocytes and the current amplitudes recorded from them. In these experiments, oocytes injected with different ranges of ZAC^{Thr128} (0.46–1.84 ng) or ZAC^{Ala128} (0.92–3.68 ng) cRNAs were incubated under the same conditions for 46–50 h before being assayed in parallel in TEVC recordings using a saturating concentration of Zn^{2+} (10 mM). For ZAC^{Thr128}-oocytes, a pronounced correlation was observed between the cRNA amount injected and the resulting recorded current amplitudes (Fig. 5D, *left*). Zn^{2+}-evoked current amplitudes in ZAC^{Ala128}-oocytes also increased somewhat with the quantity of ZAC^{Ala128} cRNA injected, but current amplitudes evoked by Zn^{2+} (10 mM) in ZAC^{Thr128}-oocytes were consistently bigger than those in ZAC^{A128}-oocytes. For example, injections of 0.92 ng and 1.84 ng cRNA gave rise to 18- and 40-fold higher amplitudes in ZAC^{Thr128}- than in ZAC^{Ala128}-oocytes, respectively, and the current amplitudes in oocytes injected with 0.46 ng ZAC^{Thr128} cRNA were 4.5-fold higher than those in oocytes injected with a 8-fold higher quantity (3.68 ng) of ZAC^{Ala128} cRNA (Fig. 5D, *left*). We further probed the importance of injected cRNA quantity for the functionality of the variant receptor in recordings of $I_{10mM\ Zn2+}$ values from oocytes injected with 42.2 ng ZAC^{Ala128} cRNA (Fig. 5D, *right*). Although injection of a 23-fold higher quantity of the ZAC variant cRNA resulted iñ2-fold higher current amplitudes in the oocytes (42.2 ng ZAC^{Ala128} cRNA: $I_{10mM\ Zn2+}$ ± S.E.M.: 0.24 ± 0.02 μA, n = 10 *versus* 1.84 ng ZAC^{Ala128} cRNA: $I_{10mM\ Zn2+}$ ± S.E.M.: 0.10 ± 0.01 μA, n = 17), notably the current amplitudes in these “high-expressing” ZAC^{Ala128}-ocytes were ~10-fold lower than those in oocytes injected with a 23-fold lower quantity of ZAC^{Thr128} cRNA (1.84 ng ZAC^{Thr128} cRNA: $I_{10mM\ Zn2+}$ ± S.E.M.: 2.37 ± 0.25 μA, n = 18) (Fig. 5D, *right*). Thus, the pronounced differences between the agonist-evoked current amplitudes through ZAC^{Thr128} and ZAC^{Ala128} in the oocytes were observed consistently over wide ranges of cRNA quantities injected into the oocytes and between oocytes injected with substantially higher quantities of cRNA encoding for the variant than for the WT receptor.

In contrast to the different agonist-evoked current amplitudes in ZAC^{Thr128}- and ZAC^{Ala128}-oocytes, the pharmacological properties displayed by the two agonists at ZAC^{Ala128} as well as the profiles of currents evoked through the variant receptor were largely comparable to those observed for ZAC^{Thr128} (Figs. 3 and 6). Zn^{2+} elicited current responses in a concentration-dependent manner in ZAC^{Ala128}-oocytes, exhibiting an averaged EC_{50} value of 620 μM (pEC_{50} ± S.E.M.: 3.21 ± 0.11, n = 7) and an averaged Hill slope of 1.27 ± 0.13 (n = 7) (Fig. 6A). Analogously to the “low-potency” H^+ concentration-response relationship observed at ZAC^{Thr128}-expressing oocytes (Fig. 3B), the H^+ concentration-response relationship at ZAC^{Ala128}-oocytes was not completed within the pH range tested (Fig. 6B). It should be noted that the apparent difference in the H^+ concentration-response relationships in Fig. 6B is a reflection of the currents having been normalised to the very different I_{pH} 4.0

Author Manuscript Author Manuscript Author Manuscript Author Manuscript

values recorded from ZAC^{Thr128}- and ZAC^{Ala128}-expressing oocytes, since H^+ applied in the pH 6.0–3.5 range evoked significant current amplitudes through both receptors. Similar to the profiles of agonist-induced current responses in ZAC^{Thr128}-oocytes (Fig. 3A–C), Zn^{2+}- and H^+-evoked currents through ZAC^{Ala128} were also characterised by a slow activation phase, very low degrees of desensitisation, and a rapid return to baseline upon termination of agonist exposure (Fig. 6A and B). However, in contrast to the significant TC-mediated suppression of the spontaneous activity in ZAC^{Thr128}-oocytes (Fig. 4C), application of TC (up to 100 μM) on its own at ZAC^{Ala128}-expressing oocytes did not produce significant apparent outward currents (data not shown). The possible reasons for this absence of measurable spontaneous activity in the ZAC^{Ala128}-oocytes will be addressed further in Section 4.

3.4. Functional properties displayed by the receptors formed in Xenopus oocytes co-expressing ZAC^{Thr128} and ZAC^{Ala128}

The high allele frequency of the c.454G>A SNP in *ZACN* means that the fraction of heterozygote individuals that carry both c.454A and c.454G alleles (and thus express both ZAC^{Thr128} and ZAC^{Ala128}) will exceed the fractions of both homozygous c.454A and homozygous c.454G carriers in almost all ethnic groups (Fig. 1D). In this light, the consequences of cells expressing both subunits for ZAC function are obviously important to consider.

In an admittedly coarse attempt to simulate the composition of the native ZAC population in heterozygous individuals carrying both c.454A and c.454G alleles and to investigate the functionality of the receptors formed in cells co-expressing ZAC^{Thr128} and ZAC^{Ala128}, we characterised the current amplitudes evoked by Zn^{2+} (10 mM) and H^+ (pH 4.0) in oocytes injected with ZAC^{Thr128}:ZAC^{Ala128} cRNA ratios of 1:3, 1:1 and 3:1 (total cRNA amount injected: 1.84 ng) and compared them to the current amplitudes recorded in oocytes injected with the corresponding quantities of ZAC^{Thr128} cRNA on its own (Fig. 7). Under the assumption that ZAC^{Thr128} and ZAC^{Ala128} subunits are able to co-assemble into pentameric complexes, co-injection of their cRNAs in oocytes will produce a heterogenous mixture of homomeric ZAC^{Thr128}, homomeric ZAC^{Ala128} and several “heteromeric” ZAC^{Thr128}/ZAC^{Ala128} assemblies with distinct subunit stoichiometries and arrangements (Fig. 7A). The relative distribution and fraction of each of these complexes within the ZAC population expressed at the cell surface of the oocyte will be determined by the injected ZAC^{Thr128}:ZAC^{Ala128} cRNA ratio and the resulting total expression levels of the two proteins in the oocyte as well as by the respective properties of the two subunits in terms of protein folding, post-translational modifications, intracellular trafficking and their ability to be incorporated into pentameric complexes in the plasma membrane.

As previously observed (Fig. 5C), a pronounced correlation existed between ZAC^{Thr128} cRNA quantities injected into oocytes and current amplitudes recorded from them, and this correlation was not significantly altered by the co-injection of ZAC^{Ala128} cRNA with ZAC^{Thr128} cRNA into the oocytes (Fig. 7B and C). Thus, the rank order of current amplitudes evoked by Zn^{2+} and H^+ in ZAC^{Thr128}:ZAC^{Ala128}-injected oocytes were “3:1′′>”1:1′′>”1:3′′ (Fig. 7B and C). For all three ratios investigated, no significant differences

Author Manuscript Author Manuscript Author Manuscript Author Manuscript

were detected between the current amplitudes evoked by Zn^{2+} or H^+ in ZAC^{Thr128}:ZAC^{Ala128}-injected oocytes and those evoked by the respective agonists in the corresponding control ZAC^{Thr128}-oocytes (Fig. 7B and C). Thus, the concomitant co-expression of ZAC^{Ala128} in the ZAC^{Thr128}:ZAC^{Ala128}-ocytes did not seem to exert a dominant negative effect on the agonist-induced current amplitudes recorded from these oocytes compared to the oocytes expressing ZAC^{Thr128} on its own.

3.5. Expression properties of ZAC^{Thr128} and ZAC^{Ala128} in mammalian cell lines

The different agonist-induced current amplitudes through ZAC^{Thr128} and ZAC^{Ala128} could be rooted in different expression levels of the receptors at the oocyte surface. To address this, we initially attempted to quantify total and surface expression levels of Flag-tagged ZAC^{Thr128} and ZAC^{Ala128} subunits in the oocytes using a biotinylation/western blotting assay essentially as previously described [39]. Since Zn^{2+} (10 mM) and H^+ (pH 4.0) evoked dramatically bigger current amplitudes in Flag--ZAC^{Thr128}-oocytes than in Flag-ZAC^{Ala128}-oocytes, and the concentration-response relationships displayed Zn^{2+} at the two receptors were also similar to those at their untagged counterparts, the insertion of the Flag epitope appeared to be functionally silent (data not shown). However, the biotinylation/western blotting experiments were inconclusive and did not shed any light on the expression properties of the WT and variant ZAC, as no significant expression of either Flag--ZAC^{Thr128} or Flag-ZAC^{Ala128} was detected in the biotinylated sample (cell surface-expression) or in the cell lysate (total expression) (data not shown). Because of this, we decided to investigate the expression properties of the two receptors in another expression system and quantified total and cell surface expression levels of HA-tagged ZAC^{Thr128} and ZAC^{Ala128} subunits transiently expressed in tsA201 cells in an enzyme-linked immunosorbent assay (ELISA).

In the HA-ZAC^{Thr128} and HA-ZAC^{Ala128} subunits, the HA epitope was introduced immediately before the first residue in the mature ZAC protein, since epitope-tagging of ZAC and other CLR subunits in this position have been reported to be functionally silent [15,33,40–42]. Analogously to the different agonist-evoked current amplitudes in oocytes expressing the two untagged ZAC subunits, Zn^{2+}- and H^+-evoked current amplitudes in HA-ZAC^{Thr128}-expressing oocytes were dramatically bigger than those in HA-ZAC^{Ala128}-oocytes, and the Zn^{2+} concentration-response relationships determined at HA-ZAC^{Thr128} and HA-ZAC^{Ala128} were similar to those at ZAC^{Thr128} and ZAC^{Ala128} (Fig. 8A).

In the ELISA, the total and cell surface expression levels of the HA-tagged proteins were determined in permeabilized (Triton-X-treated) and non-permeabilized cells, respectively. To ensure validity of the cell surface expression data obtained in the experiments, control experiments using the heteromeric 5-HT_3AB receptor were performed in parallel. In concordance with the well-established intracellular retention of 5-HT3B in the absence of 5-HT3A [43,44], expression of HA-5-HT3B on its own in tsA201 cells did not result in significant cell surface expression of the subunit, whereas non-permeabilized cells co-expressing HA-5-HT3B and 5-HT3A exhibited a robust signal in the ELISA (Fig. 8B).

The total and cell surface expression levels of HA-ZAC^{Thr128} and HA-ZAC^{Ala128} in tsA201 cells transfected with four different cDNA quantities (4.0, 1.0, 0.25 and 0.0625 μg HA-

Author Manuscript Author Manuscript Author Manuscript Author Manuscript

ZAC^{Thr128} or HA-ZAC^{Ala128} cDNA per 6-cm dish) were investigated in the ELISA (Fig. 8B). Significant levels of total and cell surface expression were detected for both HA-ZAC^{Thr128} and HA-ZAC^{Ala128} in cells transfected with the three highest cDNA quantities, whereas the expression levels of both subunits in cells transfected with 0.0625 μg cDNA per 6-cm dish were bordering on not being significant (Fig. 8B). Both total and cell surface expression levels of HA-ZAC^{Thr128} and HA-ZAC^{Ala128} in cells transfected with the same cDNA quantities of the two subunits were very similar, and the correlations between transfected cDNA quantities and both total and cell surface expression levels thus were very similar for HA-ZAC^{Thr128}- and HA-ZAC^{Ala128}-transfected cells (Fig. 8B). The putative impact of concomitant presence of the WT and variant subunit on the expression properties of both in the tsA201 cells was investigated by co-transfecting the HA-tagged version of ZAC^{Thr128} or ZAC^{Ala128} with either the untagged "other" ZAC subunit or with the ρ1 $GABA_AR$ subunit (control) (1.0:1.0 μg cDNA per 6-cm dish). The total and surface expression levels of HA-ZAC^{Thr128} in HA-ZAC^{Thr128}:ZAC^{Ala128}- and HA-ZAC^{Thr128}:ρ1-transfected tsA201 cells were similar, as were the total and surface expression levels of HA-ZAC^{Ala128} in HA-ZAC^{Ala128}:ZAC^{Thr128}- and HA-ZAC^{Ala128}:ρ1-transfected cells (Fig. 8B). In conclusion, the overall expression properties of ZAC^{Thr128} and ZAC^{Ala128} in tsA201 cells were very similar, and when co-expressed in the cells ZAC^{Thr128} and ZAC^{Ala128} did not appear to impact the expression properties of each other.

Another important issue to consider with regard to the expression properties of ZAC^{Thr128} and ZAC^{Ala128} is whether and to which extent the WT and variant subunits are able to co-assemble into "heteromeric" ZAC^{Thr128}/ZAC^{Ala128} complexes (Fig. 7A). To elucidate this, we performed a co-immunoprecipitation experiment with HA- and myc-tagged versions of ZAC^{Thr128} and ZAC^{Ala128} expressed in various combinations in HEK293 cells (Fig. 8C). Immunoprecipitation recovered consistent and comparable amounts of recombinant myc-ZAC^{Thr128} or myc-ZAC^{Ala128}, allowing for accurate comparison of the amount of HA-ZAC^{Thr128} or HA-ZAC^{Ala128} that co-immunoprecipitated. HA-ZAC^{Thr128} and HA-ZAC^{Ala128} co-immunoprecipitated equally with myc-ZAC^{Thr128}, and HA-ZAC^{Ala128} also readily co-immunoprecipitated with myc-ZAC^{Ala128} (Fig. 8C). Taken together, these data demonstrate that both ZAC^{Thr128} and ZAC^{Ala128} readily form homomeric assemblies and that the WT and variant subunits also assemble efficiently into "heteromeric" ZAC^{Thr128}/ZAC^{Ala128} complexes in HEK293 cells, and we consider this a very strong indication that the WT and variant subunits also are able to co-assemble in *Xenopus* oocytes. These results were not particular surprising, as it seems unlikely that the Thr^{128}Ala difference in this region of the ZAC subunit would interfere significantly with its assembly into pentameric complexes (Fig. 1B).

3.6. Molecular basis for the importance of residue 128 for ZAC functionality

The different current amplitudes recorded from ZAC^{Thr128}- and ZAC^{Ala128}-oocytes pinpoints the side-chain of this residue as a key structural determinant for ZAC functionality. To probe the molecular basis for this importance further, we introduced four other amino acids in this position of ZAC and characterised the functional properties exhibited by these ZAC mutants expressed in oocytes by TEVC recordings. In addition to the ZAC^{Phe128} mutant comprising an aromatic residue with very different physico-chemical properties than

Author Manuscript Author Manuscript Author Manuscript Author Manuscript

both Thr and Ala in this position, ZAC^{Ser128}, ZAC^{Val128} and ZAC^{Ile128} were also included in these studies, as they comprise the three most closely structurally related canonical amino acids to Thr and Ala with side chains that could be argued to bridge the gap between the 1-hydroxyethyl group of Thr and the methyl group of Ala (Fig. 9A).

The current amplitudes evoked by Zn^{2+} (10 mM) in ZAC^{Ser128}-, ZAC^{Val128}- ZAC^{Ile128}- and ZAC^{Phe128}-expressing oocytes were all significantly smaller than those elicited through ZAC^{Thr128} (Fig. 9B). The average $I_{10mM\ Zn2+}$ values determined at ZAC^{Ser128} and ZAC^{Val128} were 5.7- and 7.4-fold lower than that at ZAC^{Thr128} and 5.8- and 4.5-fold higher than that at ZAC^{Ala128}, respectively, and thus constituted intermediates of the current amplitudes evoked through the WT and variant receptor (Fig. 9B, *left*). The concentration-response relationship exhibited by Zn^{2+} at ZAC^{Ser128} and ZAC^{Val128} did not differ substantially from those at ZAC^{Thr128} (Fig. 9B, *right*). In contrast, the $I_{10mM\ Zn2+}$ values obtained at ZAC^{Ile128}- and ZAC^{Phe128}-oocytes were 14- and 26-fold lower than that at ZAC^{Thr128}-oocytes, respectively, and did not differ substantially from the values observed for ZAC^{Ala128} (Fig. 9B, *left*). Zn^{2+}- evoked current amplitudes through these two ZAC mutants were so minute that the concentration-response relationship for the metal ion could not be reliably determined, but the currents evoked by 1, 3 and 10 mM Zn^{2+} in oocytes expressing the two mutants were significantly higher than those in uninjected oocytes (Fig. 9B). Analogously to the pattern observed for Zn^{2+}, the average H^+ (pH 4.0)-induced current amplitudes in ZAC^{Ser128}-, ZAC^{Val128}- and ZAC^{Phe128}-expressing oocytes were 3.6-, 6.1- and 12-fold lower than that through ZAC^{Thr128}, respectively (Fig. 9C).

All in all, the structure-activity relationship observed between the different side-chains of the various residues introduced in position 128 and their impact on the Zn^{2+}- and H^+-evoked current amplitudes evoked through ZAC made intuitively sense. While substitution of the 1-hydroxyethyl group of Thr for the much smaller methyl group (Ala) or for a very different aromatic group (Phe) was detrimental for the current response size, replacement of the 1-hydroxyethyl group with the structurally more similar hydromethyl (Ser) or isopropyl (Val) groups had a smaller impact on the current amplitudes, with introduction of additional aliphatic bulk in this position in the form of an isobutyl group (Ile) reduced the agonist-induced response size further (Fig. 9A–C). With that said, the substantially bigger current amplitudes evoked through ZAC^{Thr128} than through ZAC^{Ser128} and ZAC^{Val128} also emphasised the apparent strict requirements to the composition of the side chain for ZAC functionality, with 1-hydroxyethyl being superior to even close structurally related groups.

4. Discussion

In this, the first study of ZAC expressed in *Xenopus* oocytes by TEVC electrophysiology, we have characterised and compared the functional properties of WT ZAC (ZAC^{Thr128}) and its high-frequency variant ZAC^{Ala128}. The work provides an in-depth insight into the pharmacological properties and the signalling characteristics of this atypical CLR and identifies a potentially considerable source of inter-individual variation when it comes to ZAC functions *in vivo*.

Author Manuscript Author Manuscript Author Manuscript Author Manuscript

4.1. Functional properties of ZAC signalling

The pharmacological properties exhibited by Zn^{2+}, H^+ and TC at WT ZAC as well as the signalling characteristics displayed by the channel in this study were all in all in good agreement with those observed in previous patch-clamp studies of the receptor in mammalian cells [13, 15]. Also when expressed in oocytes, ZAC exhibited significant levels of spontaneous activity, the agonist-evoked ZAC currents were easily reconcilable with a channel characterised by slow activation kinetics and by slow and minute degrees of desensitisation, and the I-V relationships of both spontaneous and agonist-induced ZAC currents were very characteristic for those of a Na^+/K^+-conducting channel (Figs. 3 and 4). TEVC recordings from oocytes proved to be a very robust assay for ZAC signalling, and in general data extracted from the recordings were very consistent, the one notable exception being the “low-potency” and “high-potency” H^+ concentration-response relationships (Fig. 3B). As outlined in Results, both of these proton-evoked responses were clearly mediated through ZAC, and the variability in H^+ potency seemed to be rooted in oocyte batch-to-batch variation as several other possible contributing factors were ruled out. Since no pronounced differences were observed between ZAC-oocytes exhibiting “high-potency” and “low-potency” H^+-profiles, be it ZAC expression levels (assessed by current amplitudes), oocyte quality or other factors, we can not explain this variability. However, it was addressed by including WT ZAC (ZAC^{Thr128}) as reference in all recordings performed in this work.

4.2. Impact of the $Thr^{128}Ala$ variation on ZAC functionality

The remarkably different current amplitudes evoked by Zn^{2+} and H^+ in ZAC^{Thr128}- and ZAC^{Ala128}-oocytes were observed consistently in experiments performed over a considerable time period using different batches of oocytes, different cRNA preparations for both subunits, and different oocyte rigs (Fig. 5A–C). These distinct functionalities were observed in recordings for up to 6 days following ZAC^{Thr128} and ZAC^{Ala128} cRNA injections in the oocytes and even in comparisons between oocytes injected with substantially higher quantities of ZAC^{Ala128} cRNA than ZAC^{Thr128} cRNA (Figs. 2D and 5C,D). Thus, the differential functional expression of the two receptors does not seem to be rooted in different time courses for processes involved in the cell surface expression of them, and the consistency of agonist-evoked current amplitudes recorded from ZAC^{Ala128}-oocytes during different experimental conditions also strongly suggests that the minute functional expression of the variant ZAC compared to the WT receptor is a general characteristic, at least for recombinant ZAC in the oocyte expression system. The apparent importance of the identity of residue 128 for ZAC expression/functionality is also strongly supported by the substantially reduced agonist-induced current amplitudes evoked through four other $ZAC^{Thr128X}$ mutants compared to ZAC^{Thr128} (Fig. 9). In contrast to this difference in current amplitudes, the pharmacological properties and signalling characteristics exhibited by WT ZAC and its high-frequency variant were very comparable. Rather than being a reflection of a real difference between ZAC^{Thr128} and ZAC^{Ala128} properties, we ascribe the apparent lack of spontaneous activity in ZAC^{Ala128}-oocytes to the overall reduced expression/functionality of the variant receptor as this most likely means that the fraction of the total response window constituted by the spontaneous activity is below the levels of detection. Importantly, the insignificant levels of spontaneous activity in ZAC^{Ala128}-oocytes also demonstrate that the $Thr^{128}Ala$ substitution has not skewed the equilibrium between the

Author Manuscript Author Manuscript Author Manuscript Author Manuscript

resting and active ZAC conformations markedly towards the latter. Thus, the minute agonist-induced current amplitudes evoked through ZAC^{Ala128} compared to ZAC^{Thr128} are not a manifestation of constitutive activity of the variant receptor making up a much higher fraction of an otherwise comparable total response window compared to the WT receptor.

The difference between the WT and variant ZAC current amplitudes in the oocytes could have several origins. Since both ZAC^{Thr128} and ZAC^{Ala128} currents are characterised by very low degrees of desensitisation (or channel block) even at high agonist concentrations, the recorded whole-cell current amplitudes in ZAC^{Thr128}- and ZAC^{Ala128}-oocytes are determined by channel conductance (γ) and open state probability (P_o) and by the number of channels in the oocyte plasma membrane (N) [45,46]. In light of the very similar pharmacological properties exhibited by Zn^{2+} and H^+ at ZAC^{Thr128} and ZAC^{Ala128}, any reduction in the channel conductance and/or open probability of ZAC brought on by the $Thr^{128}Ala$ variation would have to be completely isolated from the ability of these agonist to bind to and gate the channel. As for a putative expression-based contribution to the observed difference, the $Thr^{128}Ala$ substitution could certainly be envisioned to affect one of the many processes underlying the expression of ZAC complexes in the plasma membrane. The almost indistinguishable expression properties displayed by ZAC^{Thr128} and ZAC^{Ala128} in tsA201 cells (Fig. 8B) strongly suggest that the two subunits also could be expressed at comparable levels in the oocytes, especially in light of the high protein expression capability of this expression system. On the other hand, the mammalian tsA201 cell could possibly express co-factors facilitating optimal expression of both ZAC subunits that are not present in the oocyte. While the ELISA data taken at face value thus indicate that the different current amplitudes evoked in ZAC^{Thr128}- and ZAC^{Ala128}-oocytes arise from distinct channel conductance and/or open probability properties of the two channels, we can not completely rule out that expression differences between the WT and variant ZAC subunits in the oocytes could contribute as well.

Any interpretation of the insignificant effect that the concomitant presence of ZAC^{Ala128} has on agonist-induced current amplitudes in ZAC^{Thr128}:ZAC^{Ala128}-oocytes compared to those in the ZAC^{Thr128}-oocyte controls in the co-expression experiments (Fig. 7) will inevitably be linked to the possible origins of the differential current amplitudes exhibited by homomeric ZAC^{Thr128} and ZAC^{Ala128}. In one scenario, the co-expression data would be reconcilable with reduced oocyte surface expression of ZAC^{Ala128} compared to ZAC^{Thr128}, since the whole-cell current amplitudes in ZAC^{Thr128}:ZAC^{Ala128}-oocytes in this scenario pre-dominantly would be evoked through ZAC^{Thr128} complexes. In this connection, it should noted that the co-expression of ZAC^{Ala128} in the ZAC^{Thr128}:ZAC^{Ala128}-oocytes does not seem to retain ZAC^{Thr128} inside the cell, a finding mirrored by the co-expression results from the ELISA experiments in tsA201 cells (Fig. 8B). Interestingly, co-immunoprecipitation of recombinant ZAC from HEK293 cells (Fig. 8C) suggests that the presence of Thr or Ala in position 128 in the ZAC subunit has no impact on its ability to assemble into pentameric complexes, as the formation of “heteromeric” ZAC^{Thr128}/ZAC^{Ala128} complexes does not seem to be disfavoured compared to homomeric ZAC^{Thr128} and homomeric ZAC^{Ala128} receptors. In this “expression-based” scenario, the very similar current amplitudes evoked by agonists in ZAC^{Thr128}-and ZAC^{Thr128}:ZAC^{Ala128}-oocytes would thus have to arise from different total expression levels of the two subunits in the

Author Manuscript Author Manuscript Author Manuscript Author Manuscript

oocyte, and not from the ZAC^{Ala128} protein being somehow impaired in its trafficking to the cell surface compared to ZAC^{Thr128}.

In another scenario, homomeric WT and variant ZAC are expressed at the oocyte surface at comparable levels, and the different current amplitudes recorded from ZAC^{Thr128}-and ZAC^{Ala128}-oocytes are thus pre-dominantly arising from their respective channel properties. Considering the apparent efficient co-assembly of WT and variant ZAC subunits (Fig. 8C), this scenario would entail ZAC^{Thr128}:ZAC^{Ala128}-injected oocytes to express highly heterogenous receptor populations comprised by homomeric ZAC^{Thr128}, homomeric ZAC^{Ala128} and various stoichiometries of mixed ZAC^{Thr128}/ZAC^{Ala128} complexes (Fig. 7A), the relative fractions of these being determined by the injected cRNA ratios. The comparable agonist-evoked current amplitudes recorded in ZAC^{Thr128}:ZAC^{Ala128}-oocytes and their control ZAC^{Thr128}-oocytes could indicate that the incorporation of one or more ZAC^{Ala128} subunits together with ZAC^{Thr128} subunits ZAC^{Thr128}/ZAC^{Ala128} pentamers does not confer substantially reduced functionality compared to the ZAC^{Thr128} homomer. In other words, the absence of a dominant negative effect of ZAC^{Ala128} on the ZAC functionality in these oocytes could be interpreted to reflect that presence of ZAC^{Thr128} in these mixed complexes is sufficient to alleviate or lessen whatever impairment that the Ala^{128} residue imprints on the channel properties of the homomeric ZAC^{Ala128} complex.

4.3. Molecular basis for the importance of residue 128 for ZAC functionality

The structure-activity relationship information extractable from the agonist-evoked current responses through ZAC^{Thr128}, ZAC^{Ala128} and four additional $ZAC^{Thr128X}$ mutants points to the structural requirements to the side chain of residue 128 for optimal ZAC functionality being very strict. Replacement of the 1-hydroxyethyl moiety of Thr^{128} with very different side chains yielded very functionally compromised mutants (ZAC^{Ala128} and ZAC^{Phe128}), whereas the current amplitudes elicited through mutants comprising residues much more similar to Thr in position 128 (Ser, Val, Ile) were significantly higher, albeit still markedly lower than those evoked through ZAC^{Thr128} (Fig. 9). Not having studied other $ZAC^{Thr128X}$ mutants, we cannot claim that a Thr residue with its branched, polar/uncharged and hydrophilic side chain in this position represents the global optimum for ZAC functionality amongst the canonical amino acids. However, the detrimental effects of the conservative Thr^{128}Ser and Thr^{128}Val substitutions on ZAC functionality are striking and suggest that the superiority of the 1-hydroxyethyl side chain in this position is rooted in its branched nature and/or its β-methyl group (Thr *vs.* Ser) as well as in its hydroxy group (Thr *vs.* Val). The further reduction in functionality observed for ZAC^{Ile128} suggests that there is limited space for additional bulk in this position, even when it is added onto the β-branched side-chain scaffold (Val *vs.* Ile).

Deeper interpretation of the molecular basis for the importance of residue 128 would obviously benefit greatly from greater insight into the specific ZAC properties affected by the mutations of it. Even though the ELISA data from the tsA201 cells strongly suggests otherwise (Fig. 8B), the impact of Thr^{128} substitutions on the recorded ZAC responses could still be rooted in reduced cell surface expression of the variant/mutant receptors in the oocytes. While it seems unlikely that the lower current amplitudes recorded from all five

Author Manuscript Author Manuscript Author Manuscript Author Manuscript

$ZAC^{Thr128X}$ mutants could arise from reduced cRNA translation and lower total expression levels of the variant/mutant proteins in the oocytes, it is certainly plausible that the presence of 1-hydroxyethyl group as side-chain in position 128 could be important for the efficacy of processes in maturation and folding, post-translation modifications and/or the trafficking and the insertion of the ZAC protein in the plasma membrane. Conversely, substitutions of a residue in the β6′ segment of the ZAC ECD could also be envisioned to impact the channel characteristics of the receptor. This short β-sheet segment links the "loop E" and the Cys-loop known to be involved in the agonist binding to and the ECD/TMD crosstalk during the signal transduction through the classical CLR, respectively [2–4,8,11], and structural changes in this segment could certainly be envisioned to destabilise the β-sheet structure and induce a local structural change or to disrupt molecular interactions between residues in β6′ and in the two β4-β5 loop segments in its proximity (Fig. 1B). In support of the latter hypothesis, a study of the α7 nAChR has proposed that interactions between two residues in β6′ (corresponding to Thr^{129} and Glu^{130} in ZAC) and three residues in β4-β5 are involved in the coupling of agonist binding to gating of this receptor [47]. Although it still is unknown to which extent the mechanisms underlying agonist-evoked ZAC signalling resemble those for the classical CLR, it is tempting to speculate that residue 128 in β6′ of ZAC analogously could form intra-molecular or inter-molecular interactions of similar importance for channel properties such as open probability.

The importance of Thr^{128} for ZAC functionality seems to be supported by its evolutionary conservation across species, the degree of which exceeds the conservation of the vast majority of residues in the ZAC protein. A NCBI BLAST search finds the Thr residue to be completely conserved in all mammalian ZAC sequences published to date (from > 100 species). Interestingly, the conservation of this residue in ZAC across species also seems to extend to the classical human CLRs, with all but one of 19 $GABA_AR$ and 4 GlyR subunits comprising Thr (β GlyR: Ser), 14 of 16 nAChR subunits comprising Ile (β3/α5: Ser/Asn), and the two major 5-HT_3R subunits 5-HT3A and 5-HT3B comprising Gln (5-HT3C/5-HT3E: Arg/Lys) residues in the corresponding position. While the identity of this residue thus differs between the CLRs, its pronounced conservation across the members of each subfamily indicates that the physico-chemical properties of its side-chain also could be of functional importance for the classical CLRs, but this has to our knowledge not been investigated.

4.4. Putative impact of the Thr^{128}Ala variation on ZAC physiology

The remarkable high frequencies of this *ZACN* SNP in all ethnic groups investigated to date make it a potentially major contributor to inter-individual variation in ZAC-mediated functions. To our knowledge, there are presently no published association studies linking the Thr^{128}Ala variation in ZAC to any diseases or phenotypic traits, which could be a reflection of many things.

It is obviously important to exercise a healthy amount of caution when speculating about the putative implications of the SNP for ZAC physiology based on the observed impact of the Thr^{128}Ala variation on receptor functionality in the oocyte expression system. One aspect of this is whether and to which extent the dramatic difference in current amplitudes recorded

Author Manuscript Author Manuscript Author Manuscript Author Manuscript

from ZAC^{Thr128}-and ZAC^{Ala128}-oocytes translates into a similar difference in the current responses mediated by the native WT and variant receptors. Even though the functional characteristics exhibited by a channel in a heterologous expression system may not be mirrored completely by it *in vivo*, robust differences in the inherent channel characteristics such as conductance and open probability of the two recombinant receptors would most likely also apply for their native counterparts. If, on the other hand, the distinct current amplitudes recorded from ZAC^{Thr128}-and ZAC^{Ala128}-oocytes mainly are based in differential receptor expression, the presence of endogenous co-factors or helper proteins *in vivo* could possibly aid in processes underlying this with more comparable cell surface expression levels of the two receptors and a diminished impact of the variation *in vivo* as the result.

The putative *in vivo* effects arising from this *ZACN* SNP will inevitably depend on the specific physiological functions governed by ZAC and on the possible existence of compensatory mechanisms counteracting the impact of the Thr^{128}Ala variation in the receptor. Considering how poorly elucidated the physiological functions governed by ZAC presently are, it is difficult to predict which phenotypic traits or abnormalities that homozygous or heterozygous carriers of the c.454G allele potentially could exhibit. However, when pondering about the possible manifestation of this variation *in vivo*, it is interesting to note the existence of another high-frequency SNP in *ZACN* [c.841C>T, SNP in exon 7, rs1043149, chr17:76081716, GRCh38.p12] that has been identified in allele frequencies in the 0.10–0.20 range in a range of ethnicities in most studies (NCBI dbSNP, build 154, rs1043149 [29]) This SNP encodes for the Gln^{257}Ter variation (Gln^{281}Ter in the precursor protein) and thus yields a ZAC protein truncated at a position at the end of transmembrane α-helix M2, which is bound to be completely non-functional. The fact that no disorders or pronounced phenotypic traits so far have been linked to homozygous c.841T allele carriers, which effectively can be considered human ZAC knockouts, indicates that the *in vivo* implications of genetic disruption of ZAC signalling, if any, may be subtle. While this also would be expected to apply for the rs2257020 variation, both of these SNPs could still be envisioned give rise to distinct phenotypes within specific physiological domains. Thus, the findings in this study calls for future association studies in search for a phenotype for the rs2257020 SNP, which in addition to elucidating whether the dramatic impact of the Thr^{128}Ala variation on recombinant ZAC functionality translates into phenotypic traits also could shed light on the putative physiological roles governed by this CLR.

Acknowledgements

The work was supported by the Danish Council of Independent Research for Medical Sciences, NIH-National Institute of Mental Health grant (MH097446), and National Institute of Neurological Disorders and Stroke (NS108378, NS111064 and NS111338). Drs. Nina Braun and Mette Homann Poulsen are thanked for their kind help in connection with the biotinylation experiments.

Abbreviations:

5-HT	5-hydroxytryptamine
5-HT$_3$R	5-HT$_3$ receptor

Author Manuscript Author Manuscript Author Manuscript Author Manuscript

CLR	Cys-loop receptor
ECD	extracellular domain
ELISA	enzyme-linked immunosorbent assay
GABA	γ-aminobutyric acid
$GABA_AR$	$GABA_A$ receptor
GlyR	glycine receptor
HA	hemagglutinin
I-V	current-voltage
nAChR	nicotinic acetylcholine receptor
SNP	single nucleotide polymorphism
TEVC	two-electrode voltage clamp
TMD	transmembrane domain
ZAC	Zinc-Activated Channel

References

[1]. Alexander SPH, Mathie A, Peters JA, Veale EL, Striessnig J, Kelly E, Armstrong JF, Faccenda E, Harding SD, Pawson AJ, Sharman JL, Southan C, Davies JA, Collaborators C, THE CONCISE GUIDE TO PHARMACOLOGY 2019/20: ion channels, Br. J. Pharmacol 176 (Suppl 1) (2019) S142–S228. [PubMed: 31710715]

[2]. Hassaine G, Deluz C, Grasso L, Wyss R, Tol MB, Hovius R, Graff A, Stahlberg H, Tomizaki T, Desmyter A, Moreau C, Li XD, Poitevin F, Vogel H, Nury H, X-ray structure of the mouse serotonin 5-HT_3 receptor, Nature 512 (7514) (2014) 276–281. [PubMed: 25119048]

[3]. Du J, Lu W, Wu S, Cheng Y, Gouaux E, Glycine receptor mechanism elucidated by electron cryo-microscopy, Nature 526 (7572) (2015) 224–229. [PubMed: 26344198]

[4]. Morales-Perez CL, Noviello CM, Hibbs RE, X-ray structure of the human α4β2 nicotinic receptor, Nature 538 (7625) (2016) 411–415. [PubMed: 27698419]

[5]. Laverty D, Desai R, Uchanski T, Masiulis S, Stec WJ, Malinauskas T, Zivanov J, Pardon E, Steyaert J, Miller KW, Aricescu AR, Cryo-EM structure of the human α1β3γ2 $GABA_A$ receptor in a lipid bilayer, Nature 565 (7740) (2019) 516–520. [PubMed: 30602789]

[6]. Polovinkin L, Hassaine G, Perot J, Neumann E, Jensen AA, Lefebvre SN, Corringer PJ, Neyton J, Chipot C, Dehez F, Schoehn G, Nury H, Conformational transitions of the serotonin 5-HT_3 receptor, Nature 563 (7730) (2018) 275–279. [PubMed: 30401839]

[7]. Gharpure A, Noviello CM, Hibbs RE, Progress in nicotinic receptor structural biology, Neuropharmacology 171 (2020), 108086.

[8]. Gielen M, Thomas P, Smart TG, The desensitization gate of inhibitory Cys-loop receptors, Nat. Commun 6 (2015) 6829. [PubMed: 25891813]

[9]. Taly A, Corringer PJ, Guedin D, Lestage P, Changeux JP, Nicotinic receptors: allosteric transitions and therapeutic targets in the nervous system, Nat. Rev. Drug Discov 8 (9) (2009) 733–750. [PubMed: 19721446]

[10]. Walstab J, Rappold G, Niesler B, 5-HT_3 receptors: role in disease and target of drugs, Pharmacol. Ther 128 (2010) 146–169. [PubMed: 20621123]

Author Manuscript Author Manuscript Author Manuscript Author Manuscript

[11]. Chua HC, Chebib M, $GABA_A$ receptors and the diversity in their structure and pharmacology, Adv. Pharmacol 79 (2017) 1–34. [PubMed: 28528665]

[12]. Lynch JW, Zhang Y, Talwar S, Estrada-Mondragon A, Glycine receptor drug discovery, Adv. Pharmacol 79 (2017) 225–253. [PubMed: 28528670]

[13]. Davies PA, Wang W, Hales TG, Kirkness EF, A novel class of ligand-gated ion channel is activated by Zn^{2+}, J. Biol. Chem 278 (2) (2003) 712–717. [PubMed: 12381728]

[14]. Houtani T, Munemoto Y, Kase M, Sakuma S, Tsutsumi T, Sugimoto T, Cloning and expression of ligand-gated ion-channel receptor L2 in central nervous system, Biochem. Biophys. Res. Commun 335 (2) (2005) 277–285. [PubMed: 16083862]

[15]. Trattnig SM, Gasiorek A, Deeb TZ, Ortiz EJ, Moss SJ, Jensen AA, Davies PA, Copper and protons directly activate the zinc-activated channel, Biochem. Pharmacol 103 (2016) 109–117. [PubMed: 26872532]

[16]. Fakhfouri G, Rahimian R, Dyhrfjeld-Johnsen J, Zirak MR, Beaulieu JM, $5\text{-}HT_3$ receptor antagonists in neurologic and neuropsychiatric disorders: the iceberg still lies beneath the surface, Pharmacol. Rev 71 (3) (2019) 383–412. [PubMed: 31243157]

[17]. Juza R, Vlcek P, Mezeiova E, Musilek K, Soukup O, Korabecny J, Recent advances with $5\text{-}HT_3$ modulators for neuropsychiatric and gastrointestinal disorders, Med. Res. Rev 40 (2020) 1593–1678.

[18]. Belelli D, Hogenkamp D, Gee KW, Lambert JJ, Realising the therapeutic potential of neuroactive steroid modulators of the $GABA_A$ receptor, Neurobiol. Stress 12 (2020), 100207.

[19]. Engin E, Benham RS, Rudolph U, An emerging circuit pharmacology of $GABA_A$ receptors, Trends Pharmacol. Sci 39 (8) (2018) 710–732. [PubMed: 29903580]

[20]. Grupe M, Grunnet M, Bastlund JF, Jensen AA, Targeting α4β2 nicotinic acetylcholine receptors in central nervous system disorders: perspectives on positive allosteric modulation as a therapeutic approach, Basic Clin. Pharmacol. Toxicol 116 (2015) 187–200. [PubMed: 25441336]

[21]. Ghasemi M, Hadipour-Niktarash A, Pathologic role of neuronal nicotinic acetylcholine receptors in epileptic disorders: implication for pharmacological interventions, Rev. Neurosci 26 (2) (2015) 199–223. [PubMed: 25565544]

[22]. Terry AV Jr., Callahan PM, α7 nicotinic acetylcholine receptors as therapeutic targets in schizophrenia: update on animal and clinical studies and strategies for the future, Neuropharmacology 170 (2020), 108053.

[23]. Chang Y, Modulators of Zinc Activated Channel (US 2019/0022121 A1), Dignity Health, Phoeniz, AZ, United States, 2019.

[24]. Mudge J, Miller NA, Khrebtukova I, Lindquist IE, May GD, Huntley JJ, Luo S, Zhang L, van Velkinburgh JC, Farmer AD, Lewis S, Beavis WD, Schilkey FD, Virk SM, Black CF, Myers MK, Mader LC, Langley RJ, Utsey JP, Kim RW, Roberts RC, Khalsa SK, Garcia M, Ambriz-Griffith V, Harlan R, Czika W, Martin S, Wolfinger RD, Perrone-Bizzozero NI, Schroth GP, Kingsmore SF, Genomic convergence analysis of schizophrenia: mRNA sequencing reveals altered synaptic vesicular transport in post-mortem cerebellum, PLoS One 3 (11) (2008) 3625.

[25]. Li H, Wang F, Fei Y, Lei Y, Lu F, Guo P, Li W, Xun X, Aberrantly expressed genes and miRNAs in human hypopharyngeal squamous cell carcinoma based on RNAsequencing analysis, Oncol. Rep 40 (2) (2018) 647–658. [PubMed: 29916534]

[26]. Hernandez CC, Macdonald RL, A structural look at $GABA_A$ receptor mutations linked to epilepsy syndromes, Brain Res. 2019 (1714) 234–247. [PubMed: 30851244]

[27]. Bode A, Lynch JW, The impact of human hyperekplexia mutations on glycine receptor structure and function, Mol. Brain 7 (2014) 2. [PubMed: 24405574]

[28]. Celli J, Rappold G, Niesler B, The human serotonin type 3 receptor gene (*HTR3A-E*) allelic variant database, Hum. Mutat 38 (2) (2017) 137–147. [PubMed: 27763704]

[29]. Database of Single Nucleotide Polymorphisms (dbSNP), in: N.L.o.M Bethesda (MD): National Center for Biotechnology Information (Ed.) dbSNP Build ID: 154.

[30]. Krzywkowski K, Davies PA, Feinberg-Zadek PL, Bräuner-Osborne H, Jensen AA, A high frequency *HTR3B* variant associated with major depression dramatically augments the signaling of the human $5\text{-}HT_{3AB}$ receptor, Proc. Natl. Acad. Sci. USA 105 (2008) 722–727. [PubMed: 18184810]

Author Manuscript Author Manuscript Author Manuscript Author Manuscript

[31]. Horton RM, Hunt HD, Ho SN, Pullen JK, Pease LR, Engineering hybrid genes without the use of restriction enzymes: gene splicing by overlap extension, Gene 77 (1) (1989) 61–68. [PubMed: 2744488]

[32]. Chahine M, Bennett PB, George AL Jr., Horn R, Functional expression and properties of the human skeletal muscle sodium channel, Pflüg. Arch 427 (1994) 136–142.

[33]. Krzywkowski K, Jensen AA, Connolly CN, Bräuner-Osborne H, Naturally occuring mutations in the human 5-HT_{3A} gene profoundly impact 5-HT_3 receptor function and expression, Pharmacogenet. Genom 17 (2007) 255–266.

[34]. Kontou G, Ng SFJ, Cardarelli RA, Howden JH, Choi C, Ren Q, Santos MAR, Bope CE, Dengler JS, Kelley MR, Davies PA, Kittler JT, Brandon NJ, Moss SJ, Smalley JL, KCC2 is required for the survival of mature neurons but not for their development, J. Biol. Chem 296 (2021), 100364.

[35]. Kelley LA, Mezulis S, Yates CM, Wass MN, Sternberg MJ, The Phyre2 web portal for protein modeling, prediction and analysis, Nat. Protoc 10 (6) (2015) 845–858. [PubMed: 25950237]

[36]. Pettersen EF, Goddard TD, Huang CC, Couch GS, Greenblatt DM, Meng EC, Ferrin TE, UCSF Chimera–a visualization system for exploratory research and analysis, J. Comput. Chem 25 (13) (2004) 1605–1612. [PubMed: 15264254]

[37]. Kvist T, Hansen KB, Bräuner-Osborne H, The use of Xenopus oocytes in drug screening, Expert Opin. Drug Discov 6 (2011) 141–153. [PubMed: 22647133]

[38]. Buckingham SD, Pym L, Sattelle DB, Oocytes as an expression system for studying receptor/channel targets of drugs and pesticides, Methods Mol. Biol 322 (2006) 331–345. [PubMed: 16739734]

[39]. Chua HC, Wulf M, Weidling C, Rasmussen LP, Pless SA, The NALCN channel complex is voltage sensitive and directly modulated by extracellular calcium, Sci. Adv 6 (17) (2020) 3154.

[40]. Bracamontes JR, Li P, Akk G, Steinbach JH, Mutations in the main cytoplasmic loop of the $GABA_A$ receptor α4 and δ subunits have opposite effects on surface expression, Mol. Pharmacol 86 (1) (2014) 20–27. [PubMed: 24723490]

[41]. Gu S, Matta JA, Lord B, Harrington AW, Sutton SW, Davini WB, Bredt DS, Brain α7 nicotinic acetylcholine receptor assembly requires NACHO, Neuron 89 (5) (2016) 948–955. [PubMed: 26875622]

[42]. Jensen AB, Hoestgaard-Jensen K, Jensen AA, Elucidation of molecular impediments in the α6 subunit for in vitro expression of functional α6β4* nicotinic acetylcholine receptors, J. Biol. Chem 288 (2013) 33708–33721. [PubMed: 24085295]

[43]. Boyd GW, Doward AI, Kirkness EF, Millar NS, Connolly CN, Cell surface expression of 5-hydroxytryptamine type 3 receptors is controlled by an endoplasmic reticulum retention signal, J. Biol. Chem 278 (30) (2003) 27681–27687. [PubMed: 12750374]

[44]. Davies PA, Pistis M, Hanna MC, Peters JA, Lambert JJ, Hales TG, Kirkness EF, The 5-HT_{3B} subunit is a major determinant of serotonin-receptor function, Nature 397 (6717) (1999) 359–363. [PubMed: 9950429]

[45]. Colquhoun D, Binding, gating, affinity and efficacy: the interpretation of structure-activity relationships for agonists and of the effects of mutating receptors, Br. J. Pharmacol 125 (5) (1998) 924–947. [PubMed: 9846630]

[46]. Sigworth FJ, The variance of sodium current fluctuations at the node of Ranvier, J. Physiol 307 (1980) 97–129. [PubMed: 6259340]

[47]. Criado M, Mulet J, Castillo M, Aldea M, Sala S, Sala F, Interactions between loop 5 and β-strand β6' are involved in α7 nicotinic acetylcholine receptors channel gating, J. Neurochem 104 (3) (2008) 719–730. [PubMed: 17961148]

Author Manuscript Author Manuscript Author Manuscript Author Manuscript

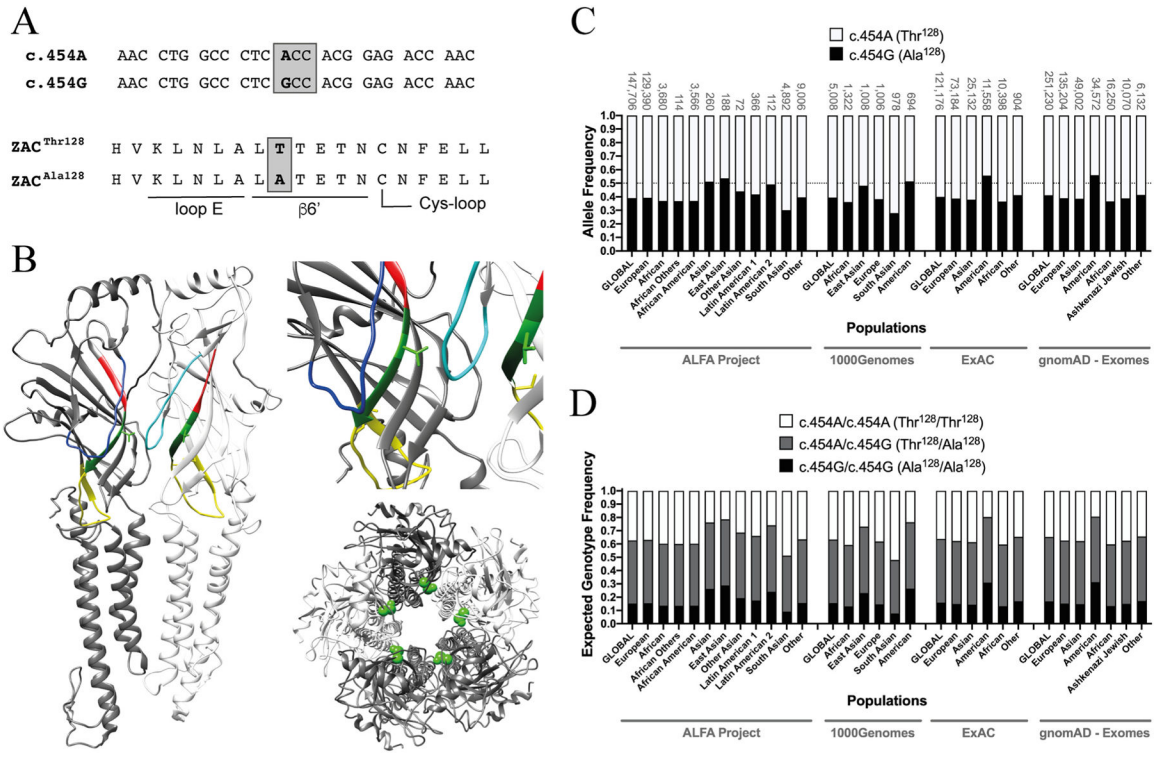

Fig. 1. The single nucleotide polymorphism c.454G>A in ZACN (rs2257020) and the resulting non-synonymous variation Thr^{128}Ala in ZAC.

A. Alignments of the nucleotide sequence segments of the c.454A and c.454G alleles of *ZACN* (*top*) comprising the variation and of the amino acid sequence segments of the ZAC^{Thr128} and ZAC^{Ala128} proteins comprising the resulting Thr^{128}Ala variation (*bottom*). The loop E and β6′ segments and part of the Cys-loop segment in ZAC are indicated. The c.454G>A SNP is given in bold, and the ACC and GCC codons encoding for Thr^{128} and Ala^{128} in ZAC, respectively, are boxed. **B**. Localisation of residue 128 (shown as Thr^{128}) in a homology model of ZAC based on the cryo-EM structure of murine 5-HT$_3$AR (PDB ID: 6HIN). *Left*: Two neighbouring subunits in the pentameric ZAC complex. The two Thr^{128} residues are shown in light-green stick, and the loop E, β6′ and Cys-loop segments are given in red, dark green and yellow, respectively. The β4-β5 loops are given in blue (dark-blue in the left subunit and light-blue in the right subunit). *Right, top*: A zoom in on Thr^{128} and its proximity in ZAC. *Right, bottom*: The ZAC complex viewed from an extracellular perspective with the Thr^{128} residues given in green spheres. **C**. Allele frequencies of the SNP c.454G>A in *ZACN* in various ethnic populations. The frequencies of the c.454A and c.454G alleles (encoding for ZAC^{Thr128} and ZAC^{Ala128}, respectively) are represented by white and black in the bars, respectively. The sample sizes of the respective ethnic populations are given above each bar, and a line marker indicates the allele frequency 0.50. The data are from the Allele Frequency Aggregator (ALFA) Project (release version 20200227123210), the 1000 Genomes Project phase3 release V3 + (1000Genomes), the Exome Aggregation Consortium (ExAC) v0.3, and the Genome Aggregation Database (gnomAD - Exomes) and have been extracted from NCBI dbSNP (build 154, rs2257020) [29], where additional reports of allele frequencies for the SNP also can be found. **D**.

Author Manuscript Author Manuscript Author Manuscript Author Manuscript

Expected frequencies of the homozygous c.454A/c.454A ($ZAC^{Thr128}/ZAC^{Thr128}$), homozygous c.454G/c.454G ($ZAC^{Ala128}/ZAC^{Ala128}$) and heterozygous c.454A/c.454G ($ZAC^{Thr128}/ZAC^{Ala128}$) genotypes in different ethnic populations. The expected genotype frequencies were calculated from the selected allele frequency data for the SNP c.454G>A in *ZACN* (rs2257020) presented in Fig. 1C using the Punnett square under the assumption of the Hardy-Weinberg theorem of Mendelian genetics in the context of populations of diploid, sexually reproducing individuals.

Author Manuscript Author Manuscript Author Manuscript Author Manuscript

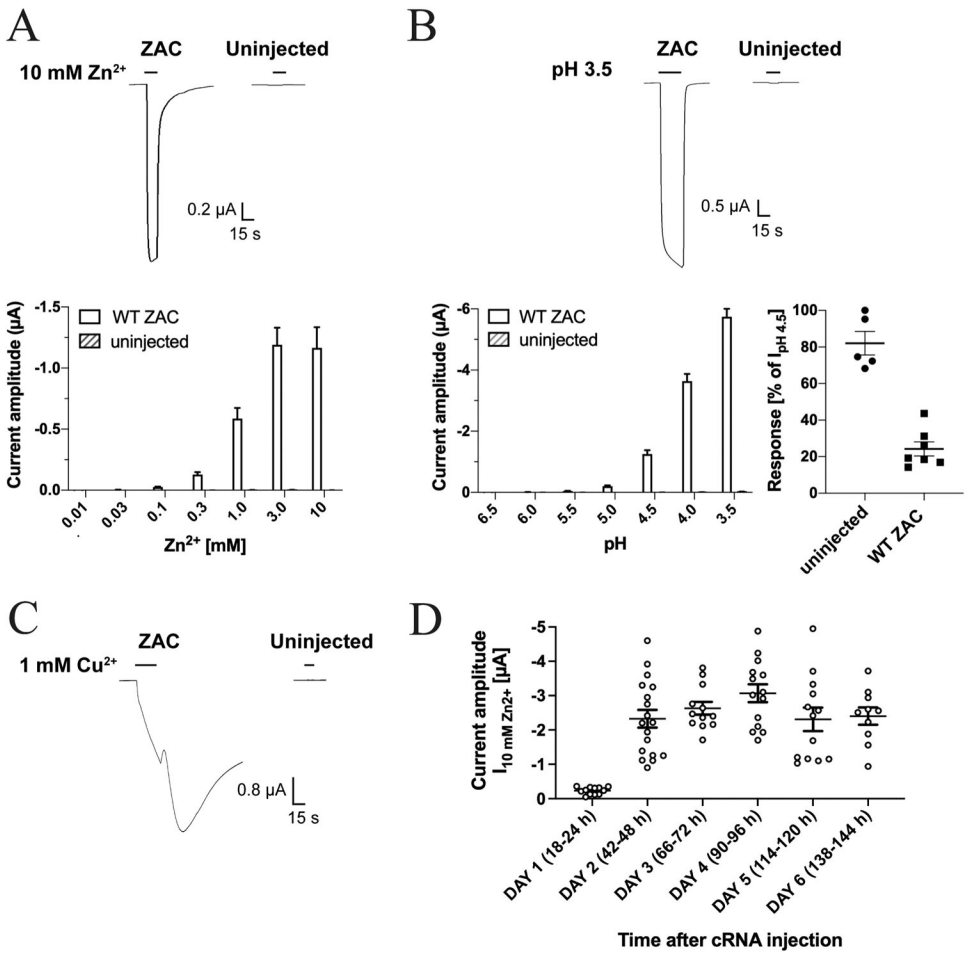

Fig. 2. Zn^{2+}-, H^{+}- and Cu^{2+}-evoked currents in oocytes injected with WT ZAC (ZAC^{Thr128}) cRNA and in uninjected oocytes.

A. Representative traces for Zn^{2+} (10 mM)-evoked currents (*top*) and averaged Zn^{2+}-evoked current amplitudes recorded from ZAC-expressing and uninjected oocytes (mean ± S.E.M., n = 8) (*bottom*). **B**. Representative traces for H^{+} (pH 3.5)-evoked currents (*top*) and averaged H^{+}-evoked current amplitudes in ZAC-expressing and uninjected oocytes (mean ± S.E.M., n = 6–7) (*bottom, left*). Inhibition of H^{+} (pH 4.5)-evoked currents in ZAC-expressing and uninjected oocytes by 100 µM tubocurarine (mean ± S.E.M, n = 5–7) (*bottom, right*). **C**. Representative traces for Cu^{2+} (1 mM)-evoked currents in ZAC-expressing and uninjected oocytes. **D**. Functional expression of ZAC in the oocytes over time. Zn^{2+}(10 mM)-evoked current amplitudes recorded from ZAC-expressing oocytes in the six days following injection of 1.84 ng cRNA into the oocytes. The specific time intervals between the cRNA injection and the recordings on Days 1–6 are indicated in parentheses. The recordings were performed on two batches of ZAC-injected oocytes, and averaged data are given as means ± S.E.M., n = 10–18).

Author Manuscript Author Manuscript Author Manuscript Author Manuscript

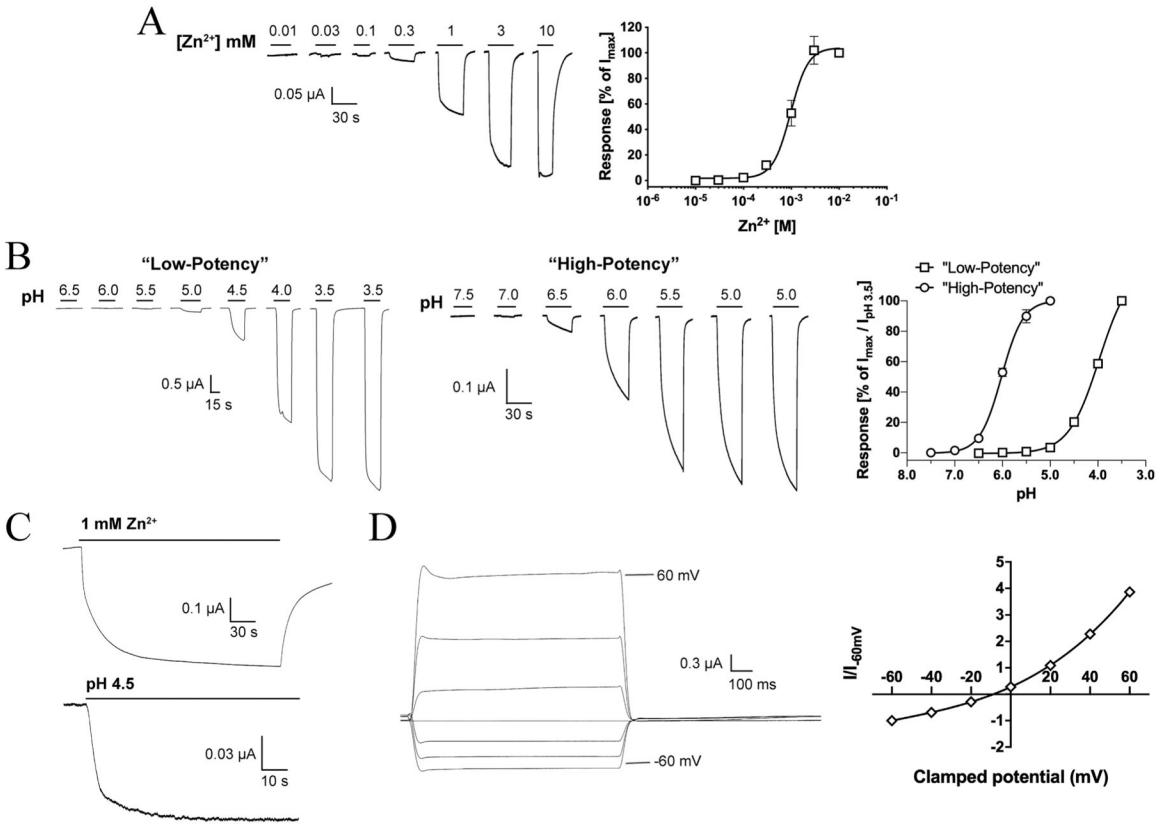

Fig. 3. Functional properties displayed by Zn^{2+} and H^+ at WT ZAC (ZAC^{Thr128}) expressed in oocytes.

A. Agonist properties of Zn^{2+}. Representative traces for Zn^{2+}-evoked currents (*left*) and averaged concentration-response relationship displayed by Zn^{2+} at ZAC (means ± S.E.M., n = 6) (*right*). **B**. Agonist properties of H^+. Representative traces for H^+-evoked currents (*left*) and averaged "low-potency" and "high-potency" concentration-response relationships displayed by H^+ at ZAC (*right*) (means ± S.E.M., n = 6–7) (*right*). The "low-potency" and "high-potency" data are normalised to the I_{pH} 3.5 value and to the fitted I_{max} value, respectively. **C**. Representative traces for currents evoked by prolonged applications of Zn^{2+} (1 mM) and H^+ (pH 4.5) at ZAC. **D**. Current-voltage (IV) relationship of Zn^{2+}-evoked currents through ZAC. Representative traces for currents evoked by prolonged application of Zn^{2+} (1 mM) at different holding potentials (*left*) and averaged IV relationship exhibited by Zn^{2+} (1 mM) at ZAC (*right*). Current amplitudes are plotted against clamped holding potentials, and data are given as leak-subtracted average current amplitudes normalised to the amplitude of currents recorded at − 60 mV (mean ± S.E.M., n = 6).

Author Manuscript Author Manuscript Author Manuscript Author Manuscript

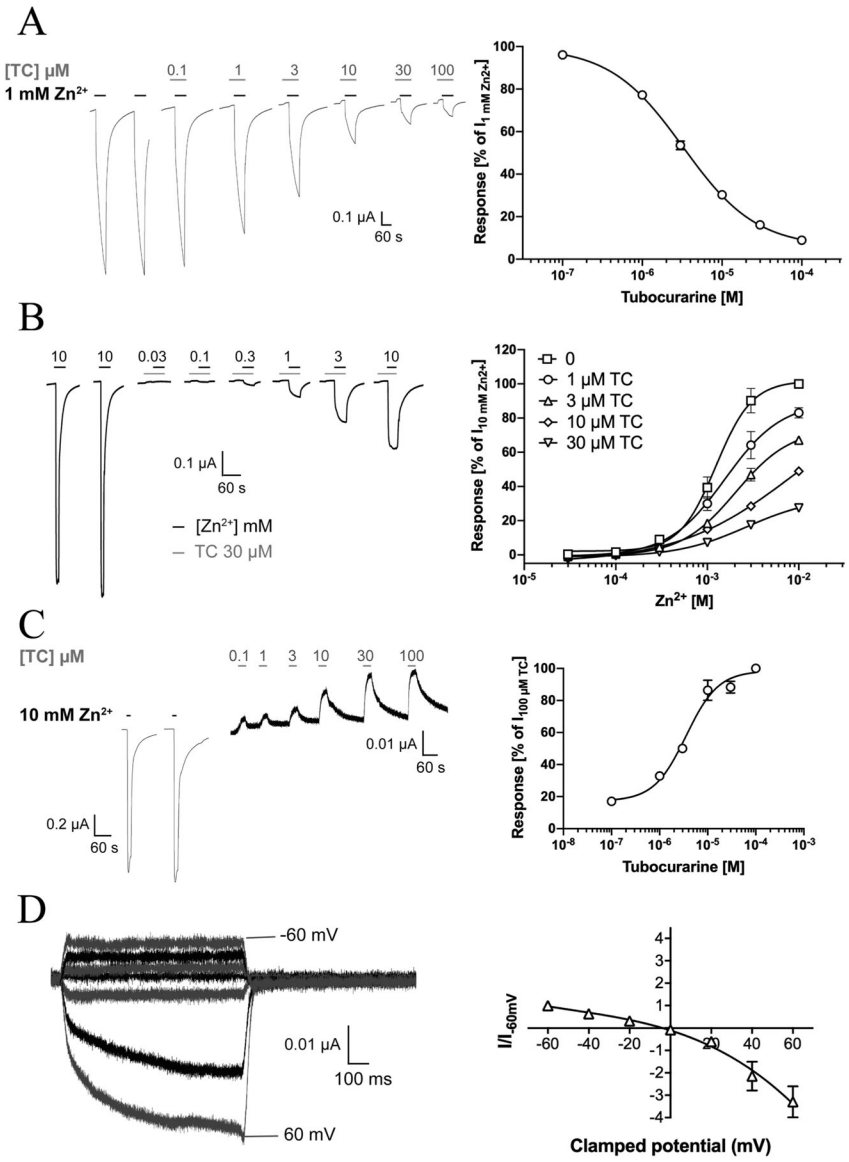

Fig. 4. Antagonist properties displayed by tubocurarine (TC) and the spontaneous activity exhibited by WT ZAC (ZAC^{Thr128}) expressed in oocytes.

A. TC-mediated inhibition of Zn^{2+}-evoked ZAC signalling. Representative traces of Zn^{2+} (1 mM)-evoked currents in ZAC-expressing oocytes in the absence and presence of increasing concentrations of TC (*left*) and averaged concentration-inhibition relationship for TC at ZAC (means ± S.E.M., n = 8) (*right*). **B**. Investigation of the mode of antagonism exerted by TC at Zn^{2+}-evoked ZAC signalling. *Left:* Representative traces for Zn^{2+}-evoked currents through ZAC in the presence of 30 µM TC. *Right:* Averaged concentration-response relationships displayed by Zn^{2+} at ZAC in the absence and in the presence of TC (1–30 µM). Data are normalised to the current evoked by 10 mM Zn^{2+} in the absence of TC ($I_{10mM\ Zn2+}$) in the oocyte (means ± S.E.M., n = 5–8). **C**. TC-mediated inhibition of the spontaneous activity of ZAC. Representative traces of the effects of increasing concentrations of TC on the leak current in ZAC-expressing oocytes (*left*) and averaged concentration-inhibition relationship for TC at the spontaneous ZAC currents in the oocytes (*right*) (means ± S.E.M.,

Author Manuscript Author Manuscript Author Manuscript Author Manuscript

n = 6). **D**. Current-voltage (IV) relationship of currents evoked by the TC-mediated block of the spontaneous ZAC activity. Representative traces for currents evoked by prolonged application of TC (100 μM) at different holding potentials (*left*), and the averaged IV relationship exhibited by TC (100 μM) at ZAC (*right*). Current amplitudes are plotted against clamped holding potentials, and data are given as leak-subtracted average current amplitudes normalised to the amplitude of currents recorded at − 60 mV (mean ± S.E.M., n = 6).

Author Manuscript Author Manuscript Author Manuscript Author Manuscript

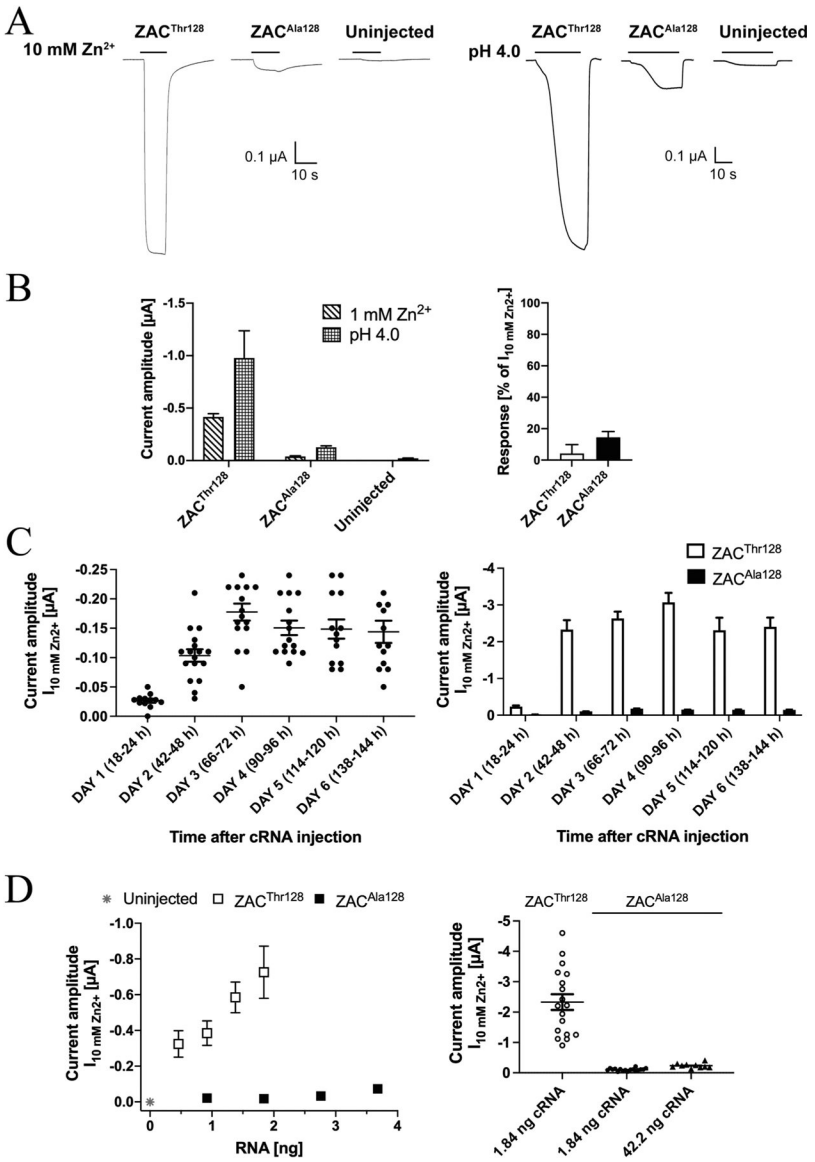

Fig. 5. Functional properties displayed by Zn^{2+} and H^+ at ZAC^{Ala128} expressed in oocytes.

A. Representative traces for the current responses evoked by Zn^{2+} (10 mM) and H^+ (pH 4.0) in ZAC^{Thr128}- and ZAC^{Ala128}-expressing oocytes (injected with 1.84 ng cRNA) and in uninjected oocytes. **B**. *Left:* Averaged current amplitudes evoked by Zn^{2+} (1 mM) and H^+ (pH 4.0) in ZAC^{Thr128}- and ZAC^{Ala128}-expressing oocytes (injected with 1.84 ng cRNA) and in uninjected oocytes (mean ± S.E.M., n = 4–7). *Right:* Averaged data for the inhibition of Zn^{2+} (10 mM)-evoked currents in ZAC^{Thr128}- and ZAC^{Ala128}-expressing oocytes mediated by TC (100 μM) (mean ± S.E.M., n = 4–6) (*right*). **C**. Functional expression of ZAC^{Ala128} in the oocytes over time. *Left:* Zn^{2+}(10 mM)-evoked current amplitudes recorded from ZAC^{Ala128}-expressing oocytes in 6 days following injection of 1.84 ng cRNA into the oocytes. The specific time intervals between the cRNA injection and the recordings on Days 1–6 are indicated in parentheses. The recordings were performed on two batches of ZAC-injected oocytes, and averaged data are given as means ± S.E.M., n = 13–17). *Right:* The

Author Manuscript Author Manuscript Author Manuscript Author Manuscript

averaged data for ZAC^{Ala128} are given together with the averaged data for ZAC^{Thr128} (also shown in Fig. 2D) for comparison. The ZAC^{Thr128} and ZAC^{Ala128} data were obtained in parallel recordings using the same two oocyte batches. **D**. *Left:* Relationship between cRNA quantities injected and the averaged current amplitudes evoked by 10 mM Zn^{2+} ($I_{10mM\ Zn2+}$) in ZAC^{Thr128}- and ZAC^{Ala128}-expressing oocytes and in uninjected oocytes (mean ± S.E.M., n = 6–12). *Right:* Zn^{2+} (10 mM)-evoked current amplitudes in oocytes injected with 1.84 ng ZAC^{Thr128} cRNA or with 1.84 ng or 42.2 ng ZAC^{Ala128} cRNA. The averaged data are given as means ± S.E. M., n = 10–18). The data for ZAC^{Thr128} (1.84 ng) and ZAC^{Ala128} (1.84 ng) are the data also shown in Figs. 2D and 5C, respectively, and the data for ZAC^{Ala128} (42.2 ng) were obtained in parallel in recordings 2 days after cRNA injection using the same two oocyte batches.

Author Manuscript Author Manuscript Author Manuscript Author Manuscript

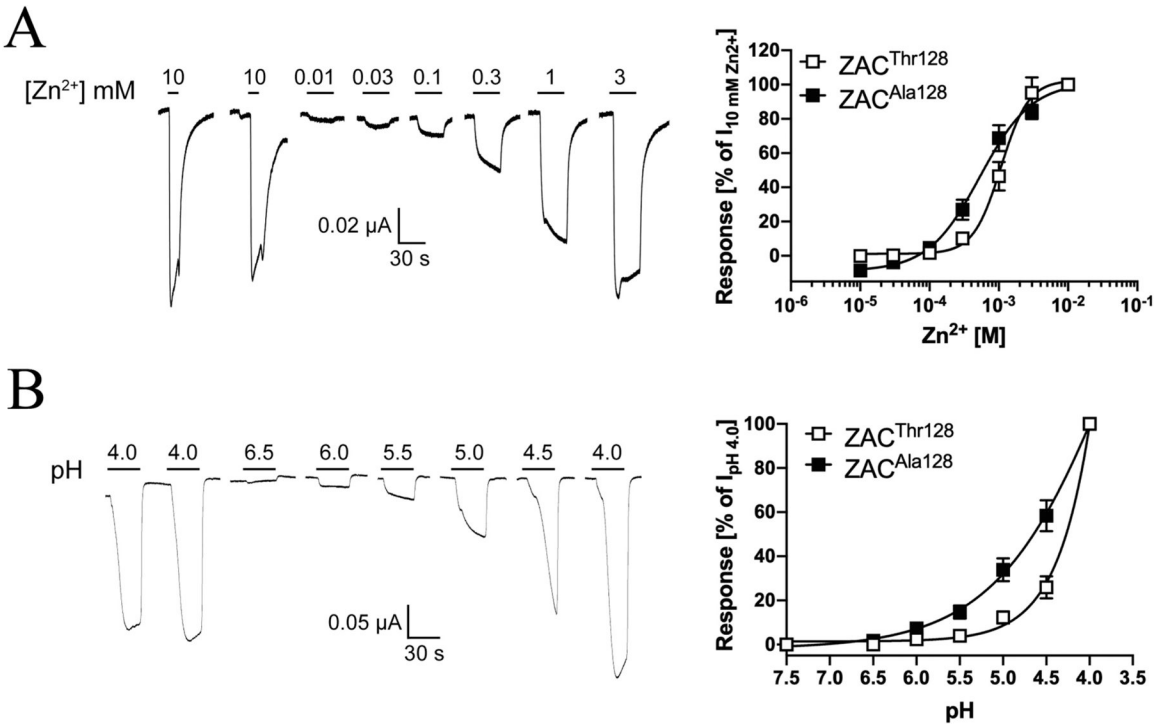

Fig. 6. Agonist pharmacology displayed by Zn^{2+} and H^+ at ZAC^{Ala128} expressed in oocytes

A. Agonist properties displayed by Zn^{2+} at ZAC^{Ala128}. Representative traces for Zn^{2+}-evoked currents in ZAC^{Ala128}-expressing oocytes (*left*) and averaged concentration-relationships for Zn^{2+} at ZAC^{Thr128} and ZAC^{Ala128} (means ± S.E.M., n = 7–8) (*right*). **B**. Agonist properties displayed by H^+ at ZAC^{Ala128}. Representative traces for H^+-evoked currents in ZAC^{Ala128}-expressing oocytes (*left*) and averaged concentration-relationships for H^+ at ZAC^{Thr128} and ZAC^{Ala128} (means ± S.E.M., n = 6) (*right*).

Author Manuscript Author Manuscript Author Manuscript Author Manuscript

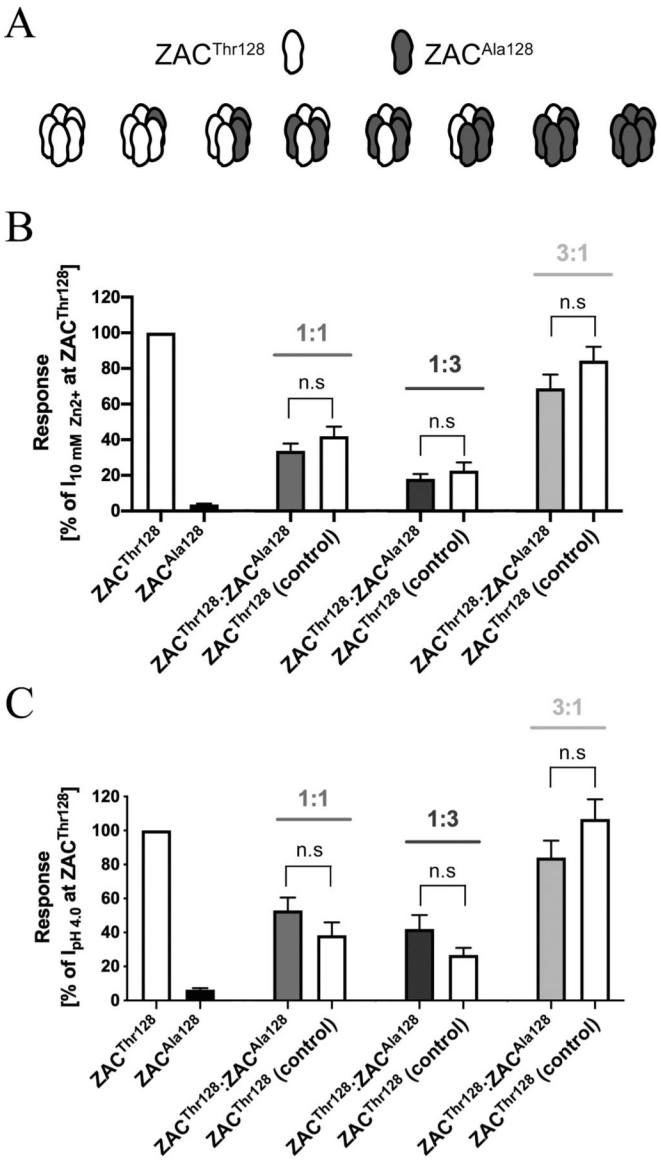

Fig. 7. Functional properties displayed by the receptors formed in Xenopus oocytes co-expressing ZAC^{Thr128} and ZAC^{Ala128}.

A. All putative combinations of ZAC pentamers that potentially can be assembled in oocytes co-expressing ZAC^{Thr128} and ZAC^{Ala128} subunits. **B,C**. Averaged current amplitudes evoked by Zn^{2+} (10 mM) (**B**) and H^+ (pH 4.0) (**C**) in ZAC^{Thr128}- and ZAC^{Ala128}-oocytes (injected with 1.84 ng cRNA), in oocytes injected with ZAC^{Thr128}:ZAC^{Ala128} cRNA ratios of 1:1, 1:3 and 3:1 (0.92:0.92 ng, 0.46:1.38 ng, 1.38:0.46 ng, respectively), and in the control oocytes injected with the corresponding ZAC^{Thr128} cRNA quantities (0.92 ng, 0.46 ng, 1.38 ng) (mean ± S.E.M., n = 7–12). Statistical analysis was performed using one-way ANOVA followed by Tukey's multiple comparisons test. Statistical values for the comparisons of Zn^{2+} (10 mM)-evoked current amplitudes: *1:1 ratio:* $P = 0.8355$, *1:3 ratio:* $P = 0.8990$, *3:1 ratio:* $P = 0.9975$, $F(7,63) = 18.71$. Statistical values for the comparisons of H^+ (pH 4.0)-evoked current amplitudes: *1:1 ratio:* $P = 0.8657$, *1:3 ratio:* $P = 0.8373$, *3:1 ratio:* $P = 0.3657$, $F(7,47) = 24.49$. *n.s.* indicates non-significant difference ($P > 0.05$).

Author Manuscript Author Manuscript Author Manuscript Author Manuscript

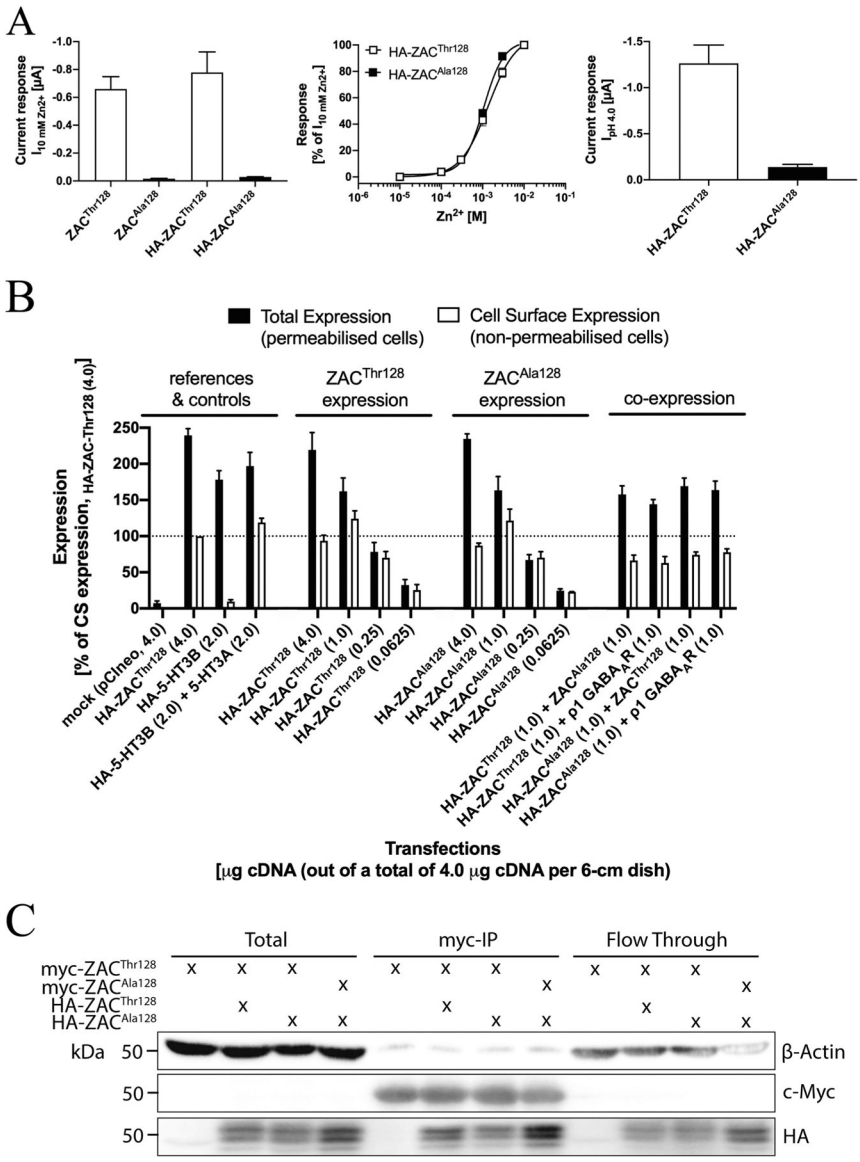

Fig. 8. Expression properties of ZAC^{Thr128} and ZAC^{Ala128} in tsA201 and HEK293 cells.

A. Functional properties of HA-ZAC^{Thr128} and HA-ZAC^{Ala128} expressed in oocytes injected with 1.84 ng cRNA of both subunits. *Left:* Averaged current amplitudes evoked by Zn^{2+} (10 mM) in ZAC^{Thr128}-, ZAC^{Ala128}-, HA-ZAC^{Thr128}- and HA-ZAC^{Ala128}-expressing oocytes (mean ± S.E.M., n = 4–8). *Middle*: Averaged concentration-response relationships displayed by Zn^{2+} at HA-ZAC^{Thr128} and HA-ZAC^{Ala128} (means ± S.E.M., n = 6–8). *Right:* Averaged current amplitudes evoked by H^+ (pH 4.0) in HA-ZAC^{Thr128}- and HA-ZAC^{Ala128}-expressing oocytes (means ± S.E.M., n = 6–8). **B**. Total and cell surface expression levels of HA-ZAC^{Thr128} and HA-ZAC^{Ala128} transiently expressed in tsA201 cells in the ELISA experiments. All transfections used a total of 4 µg cDNA (all in the pCIneo vector) per 6-cm dish, where the quantities of specific cDNAs indicated in the figure were supplemented with "empty" pCIneo up to 4 µg. Total and cell surface expression was determined in permeabilized (Triton-X-treated) and non-permeabilized cells, respectively. Data (in %,

Author Manuscript Author Manuscript Author Manuscript Author Manuscript

normalised to the absorbance for the reference "HA-ZAC^{Thr128} (4.0)"-transfected cells) are given as mean ± S.E.M. and are based on a total of three experiments (n = 3). A line marker indicates the 100% level. **C**. Co-immunoprecipitation of ZAC^{Thr128} and ZAC^{Ala128}. HEK293 cells were transfected with myc-ZAC^{Thr128} alone, myc-ZAC^{Thr128}/HA-ZAC^{Thr128}, myc-ZAC^{Thr128}/HA-ZAC^{Ala128}, or myc-ZAC^{Ala128}/HA-ZAC^{Ala128}. ZAC proteins were immunoprecipitated using myc-beads. Lysates and immunoprecipitated samples were resolved by SDS-PAGE. The myc-, HA- and actin-expression levels were measured by immunoblot.

Author Manuscript Author Manuscript Author Manuscript Author Manuscript

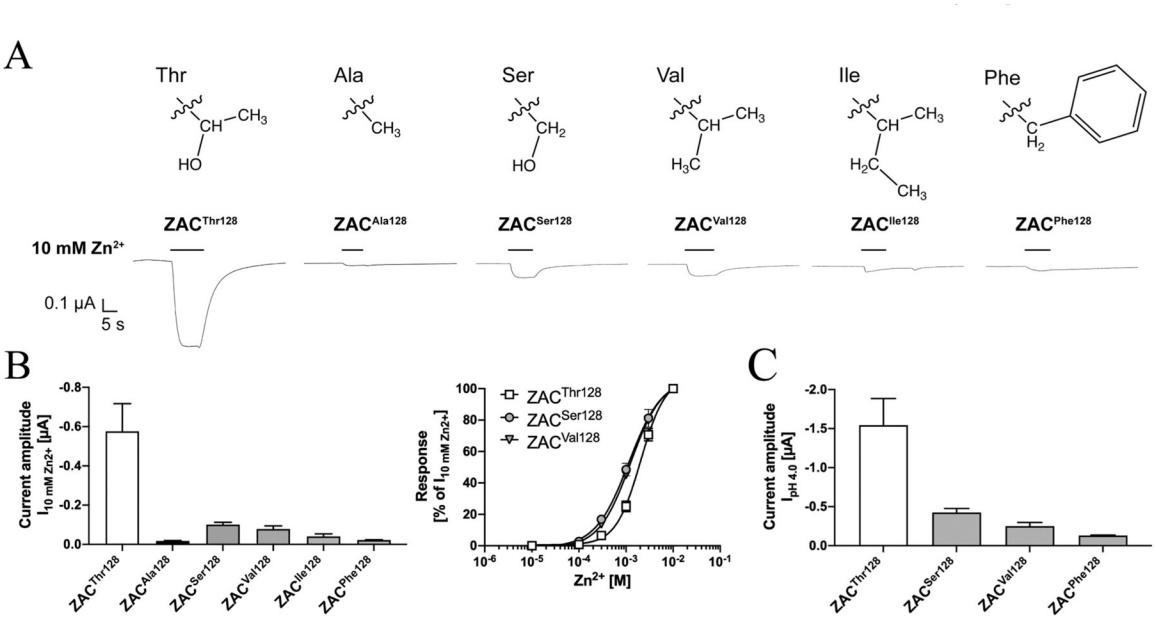

Fig. 9. Functional properties displayed by Zn^{2+} and H^+ at ZAC^{Ser128}, ZAC^{Val128}, ZAC^{Ile128} and ZAC^{Phe128} mutants expressed in oocytes.

A. The chemical structures of the side chains of the Thr, Ala, Ser, Val, Ile and Phe residues and representative traces for the current responses evoked by Zn^{2+} (10 mM) in ZAC^{Thr128}-, ZAC^{Ala128}-, ZAC^{Ser128}-, ZAC^{Val128}-, ZAC^{Ile128}- and ZAC^{Phe128}-expressing oocytes. **B**. Averaged current amplitudes evoked by Zn^{2+} (10 mM) in ZAC^{Thr128}-, ZAC^{Ala128}-, ZAC^{Ser128}-, ZAC^{Val128}, ZAC^{Ile128}- and ZAC^{Phe128}-expressing oocytes (mean ± S.E.M., n = 5–8) (*left*), and averaged concentration-relationships displayed by Zn^{2+} at ZAC^{Thr128}, ZAC^{Ser128} and ZAC^{Val128} (means ± S.E.M., n = 5–8) (*right*). **C**. Averaged current amplitudes evoked by H^+ (pH 4.0) in ZAC^{Thr128}-, ZAC^{Ser128}-, ZAC^{Val128}, and ZAC^{Phe128}-expressing oocytes (mean ± S.E.M., n = 6–8). **A–C**. All oocytes were injected with 1.84 ng cRNA of the respective ZAC subunits.